Biophysical Chemistry 4 (1976) 319–342

ELECTROSTATIC INTERACTIONS AT CHARGED LIPID MEMBRANES. I. EFFECTS OF pH AND UNIVALENT CATIONS ON MEMBRANE STRUCTURE

Hermann TRÄUBLE, Max TEUBNER, Paul WOOLLEY and Hansjörg EIBL
Max-Planck-Institut für Biophysikalische Chemie, D-34 Göttingen-Nikolausberg, Germany

Received 26 November 1975
Revised manuscript received 15 March 1976

Electrostatic interactions at charged lipid membranes make a significant contribution to the free energy of the system, and can be varied within a wide range by alteration either of the membrane's surface charge density or of the concentration of electrolytes in the surrounding medium. Changes in the charged membrane's structure, such as the ordered ⇄ fluid phase transition, can thus be induced at constant temperature by variations in pH and salt concentration. An adequate quantitative description of these phenomena is obtained from the Gouy–Chapman theory. The good agreement between theory and experiment confirms that the expression derived for the electrostatic free energy, especially in respect of its positive sign, is correct. The classical expression for the "free energy of the double layer" derived by Verwey and Overbeek, which has a negative sign, is not applicable to lipid membranes with ionizable polar groups.

1. Introduction

The structure of lipid membranes and biomembranes of fixed chemical composition depends on a number of physical factors such as temperature, pressure, pH, ions present, etc. In this respect the situation is much the same as for many biopolymers [1–4].

It is the purpose of this paper to present a detailed theoretical and experimental study of the environmental factors that affect the structure of charged membranes by way of electrostatic interactions at the membrane surface. Experimental studies were performed with membranes whose lipids carried one dissociable proton at their polar groups. Thus the surface charge and the electrostatic free energy of the membranes could be manipulated by altering the degree of dissociation, i.e. by acid–base titration, or by altering the ionic strength.

The rôle of electrostatic interactions as structure-determining factors has been studied in considerable detail, both experimentally and theoretically, for biopolymers (nucleic acids and polyaminoacids). For example, nucleic acids are anionic polyelectrolytes which carry negative charges at neutral pH owing to the presence of ionized phosphate groups. At low ionic strength electrostatic repulsion prevents the formation of compact ordered structures. Increasing ionic strength reduces the electrostatic energy and may cause transitions to more ordered structures. Another example is poly-L-glutamic acid, which shows pH- and ionic-strength-dependent transitions between helix and coil conformations. Here increasing charges induce a transition from the helix to the coil form, which begins at about 40% ionization. The reason for this behaviour is that the charges repel each other, counteracting helix-stabilizing factors.

Only recently has it been shown that analogous effects exist with charged lipid membranes and that electrostatic interactions at the membrane surface may cause transitions between different membrane structures [5–10]. As in the case of biopolymers the electrostatic surface phenomena may be divided into three sorts: (a) nonspecific screening effects that stabilize the charged surface by the formation of an ionic atmosphere (diffuse electrical double layer) at the membrane surface; (b) shifts in the apparent pK due to the influence of surface charges and of the ionic strength on the ionization of surface groups; (c) specific effects due to the binding of counterions. Here we will consider the nonspecific effects (a) and (b) only. Specific counterion binding will be the topic of a subsequent paper.

A convenient way to explore the effects of electro-

static interactions on membrane structure is to study their influence on the transition between the so-called ordered (or condensed) and fluid (or expanded) states of lipid membranes. The physical properties of these two states are reviewed by Chapman [11], Träuble and Haynes [12], Tardieu et al. [13], Seelig and Niederberger [14], and Levine [15]. The treatment which follows rests solely on the fact that in the fluid state the lipid molecules occupy a larger molecular area; as indicated by X-ray analysis [13, 16] and spin label studies (Marsh [17]) the difference in area is about 30%. This has the consequence that the electrostatic interactions between the lipid polar groups are smaller in the fluid state than in the condensed state.

The thermodynamic stability of the two membrane states may be characterized by the temperature of transition, T_t, under specified conditions of pressure, pH, ionic strength etc. As has been shown in previous papers (Träuble and Eibl [6, 7]) the presence of surface charges lowers the stability of the ordered state more than that of the fluid state and thus leads to a lowering of the transition temperature. In addition a change in ionic strength can also alter differentially the free energies of the two states (by one of the mechanisms mentioned above) and cause a shift in the transition temperature.

In the following we will present a theoretical and experimental investigation of these phenomena starting with a general survey of the theory (section 2). (See also the accompanying paper by F. Jähnig [40].) Section 3 describes the synthesis of the lipid employed. The experiments are presented in section 4. Theory and experiment are then compared in section 5, and a general discussion along with a statement of conclusions is given in section 6.

2. Theory

As will be shown in section 2.1, the effect of electrostatic interactions on the temperature of the ordered ↔ fluid transition of charged lipid membranes may be expressed as

$$T_t = T_t^* + \Delta G^{el}/\Delta S^* = T_t^* + \Delta T_t\,, \qquad (1)$$

where T_t^* denotes the transition temperature of an uncharged, but otherwise identical membrane; ΔG^{el} is the difference in molar electrostatic free energy between the fluid and the ordered states; ΔS^* is the entropy difference between the fluid and ordered states of the *uncharged* membrane. We will show that ΔG^{el} is negative, which means that the surface charges have a greater "destabilizing" effect on the ordered (condensed) state than on the fluid (expanded) state, resulting in a decrease of T_t.

2.1. Derivation of eq. (1)

To derive eq. (1) we apply a method similar to that used by Record [2] to account for electrostatic effects on structural transitions of charged biopolymers. The ordered ↔ fluid transition of lipid membranes is considered as a reversible two-state process occurring at a temperature T_t. Therefore at T_t

$$\underset{\text{(ordered, or condensed phase)}}{\text{A}} \rightleftharpoons \underset{\text{(fluid, or expanded phase)}}{\text{B}}$$

whereby we neglect the fact that the transition in general occurs over a finite temperature range. In this model the molar Gibbs free energies of the two forms, G_A and G_B, with respect to an arbitrary standard state, are equal at T_t:

$$G_A = G_B \quad \text{at } T_t\,, \qquad (2)$$

with $G_A = H_A - TS_A$ and $G_B = H_B - TS_B$; H denotes the enthalpy and S the entropy. This leads to

$$T_t = (H_B - H_A)/(S_B - S_A) = \Delta H/\Delta S\,. \qquad (3)$$

The ordered → fluid transition is an endothermic process ($\Delta H > 0$); ΔH increases with increasing hydrocarbon chain length, and has a value around 9 kcal/mole for dipalmitoyllecithin [11, 18]. The fluid state B has, of course, a higher entropy value, on account of its greater structural disorder. For dipalmitoyllecithin with $T_t = 41°C$ ΔS^* is 27.6 cal/deg mole [11].

It is next assumed that the molar free energies of the two states are composed of additive non-electrostatic and electrostatic terms. Thus for state A

$$G_A = G_A^* + G_A^{el}\,, \qquad (4)$$

with $G_A^* = H_A^* - TS_A^*$ for the non-electrostatic contributions in an uncharged system. Analogous expressions apply for state B.

Using expression (4) we obtain from condition (2)

$$\Delta G^{el} = G_B^{el} - G_A^{el} = G_A^* - G_B^* ,$$

or

$$\Delta G^{el} = -\Delta H^* + T_t \Delta S^* , \qquad (5)$$

where $\Delta H^* = H_B^* - H_A^*$ and $\Delta S^* = S_B^* - S_A^*$.

Rearranging eq. (5) leads to eq. (1):

$$T_t = \Delta H^*/\Delta S^* + \Delta G^{el}/\Delta S^* = T_t^* + \Delta T_t ,$$

where T_t^* equals $\Delta H^*/\Delta S^*$, the transition temperature of the uncharged system. $\Delta T_t = \Delta G^{el}/\Delta S^*$ denotes the shift in T_t due to electrostatic interactions. This is set out diagrammatically in fig. 4a.

We make here the assumptions (a) that in a given state (A or B) the presence of surface charges induces no structural alterations, and (b) that the assumed uncharged reference state and the protonated lipid membrane are thermodynamically identical. We also make the approximation that changes in ΔH^*, ΔS^* and ΔG^* due to their temperature dependence are negligible.

2.2. Calculation of the electrostatic free energy G^{el} and its effect on the transition temperature

2.2.1. Relation between ΔG^{el} and the change in surface area

To calculate ΔG^{el}, the change in electrostatic free energy at the ordered → fluid transition, we assume that this change is exclusively a result of the expansion of the membrane at constant charge per polar group. This assumption is justified in appendix A1. Denoting with f_A and f_B the molecular areas occupied in the plane of the membrane by the lipid molecules in states A and B respectively, we may write $\Delta f = f_B - f_A$ for the increase in molecular area at the ordered → fluid transition. In principle the value of Δf can be obtained from X-ray studies: it will be considered as an adjustable parameter in the following because X-ray studies on the system used are not yet available.

Denoting with ϕ the surface density of electrostatic free energy of the membrane we can write for each state the molar surface electrostatic free energy as

$$G^{el} = L f \phi , \qquad (6)$$

where L is Avogadro's number. ϕ is a function of the charge density σ, which in turn depends on the packing density of the lipid molecules, or on the molecular area f, i.e. $\phi = \phi(f)$.

The difference in G^{el} between states B and A is therefore

$$\Delta G^{el} = L[f_B \phi_B - f_A \phi_A] . \qquad (7)$$

To arrive at an analytical expression for ΔG^{el} we expand G^{el} in a Taylor series around state A regarding G^{el} as a function of f. This gives

$$G_B^{el} = G_A^{el} + \left.\frac{dG^{el}}{df}\right|_A \Delta f + \frac{1}{2}\left.\frac{d^2G^{el}}{df^2}\right|_A (\Delta f)^2 + \dots . \qquad (8)$$

As will be seen below (cf. fig. 4b) G^{el} is a slowly-varying function of f and therefore the first-order term is expected to be a good representation of ΔG^{el} – although the change in f at the transition is about 20–30%.

Using eq. (6) and neglecting higher-order terms yields

$$\Delta G^{el} = G_B^{el} - G_A^{el} = L(\phi + f\, d\phi/df)\, \Delta f . \qquad (9)$$

Here we have omitted the index for state A because the series expansion could have been performed equally well about state B. Therefore in the later application of eq. (9) we will use values for ϕ and $f\, d\phi/df$ that are intermediate between those for states A and B.

2.2.2. The Gouy–Chapman model

To derive an explicit expression for G^{el} we will have to calculate the surface electrostatic free energy ϕ of the membrane arising from interactions within the system of surface charges and mobile ions in solution. This will be done on the basis of the Gouy–Chapman theory of the electrical double layer [19,20]. This theory has been reviewed by Verwey and Overbeek [21], Overbeek [22], Davies and Rideal [23], Haydon [24], Adamson [25], Sanfeld [26], and Aveyard and Haydon [27]. The major assumptions made in this theory are (1) the membrane surface is regarded as a plane surface bearing a uniform charge density σ, and (2) the ions are treated as point charges *.

The ion distribution near the surface and the electrical potential Ψ are then calculated by solving the Poisson–Boltzmann equation for this system. Fig. 1 shows schematically the distribution of counterions in the diffuse layer near a negatively charged surface, and the effect of a membrane expansion (or a decrease in

* The assumptions and simplifications made in the Gouy–Chapman theory have been discussed extensively in the literature and numerous corrections have been proposed [24, 26, 28–30].

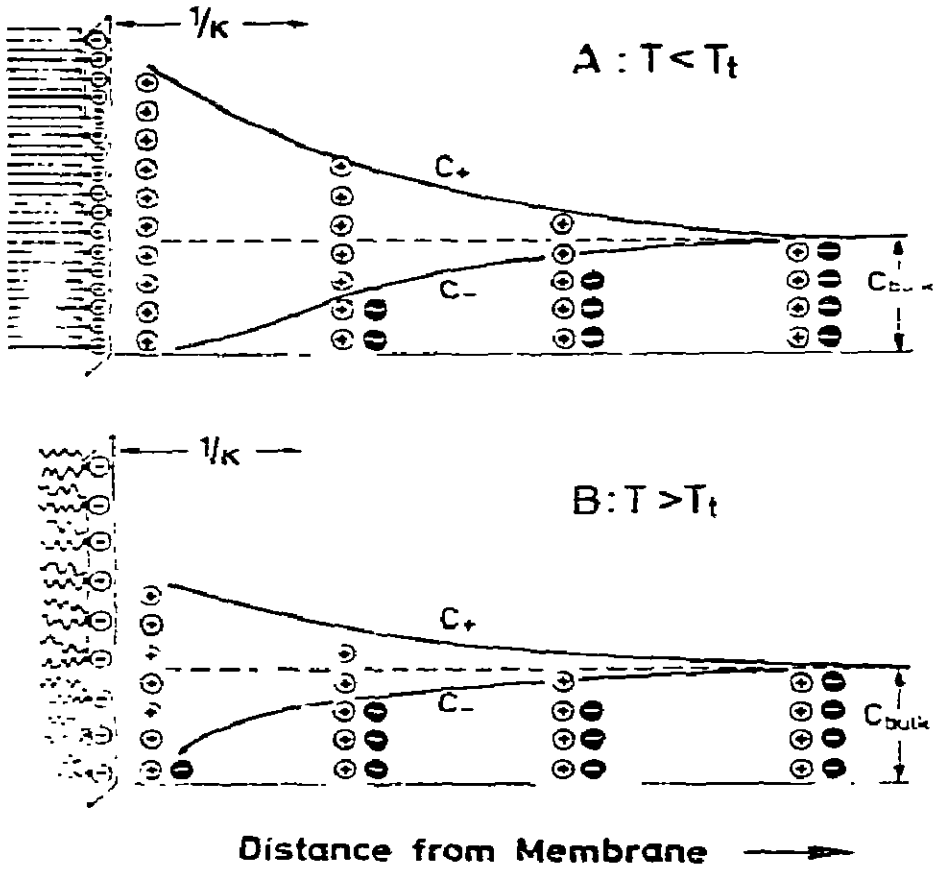

Fig. 1. The electrical double layer at a negatively-charged lipid membrane in the condensed (A) and the expanded (B) state. c_+ and c_- are the local concentrations of the cations and anions of a 1:1 electrolyte. $1/\kappa$ characterizes the thickness of the diffuse layer; $1/\kappa$ remains the same in cases A and B as its value depends only on c_{bulk}. The ordinate represents ion concentrations. (A): $T < T_t$, condensed state; surface charge density and potential high, cation build-up and anion depletion at surface large. (B): $T > T_t$, membrane expanded; surface charge density and potential low, cation build-up and anion depletion small. In both cases the area between the two concentration curves equals the density of the surface charges on the membrane, indicated on the left by the head-groups occupying a "unit area" in each of the two states.

charge density) on the diffuse layer as it occurs at the ordered → fluid transition.

With increasing salt concentration the diffuse layer is "compressed", or the counterions concentrate more and more near the membrane surface. A parameter κ is used to characterize the "thickness" of the diffuse layer. For 1:1 electrolytes κ is given by

$$\kappa^2 = (8\pi/\epsilon)(e^2/kT)n\,. \qquad (10a)$$

Here ϵ = dielectric constant, e = elementary charge, k = Boltzmann's constant and T = absolute temperature. n denotes the salt concentration in the bulk solution in molecules per cm^3; for the 1:1 electrolytes used in this study salt concentration and ionic strength are equal.

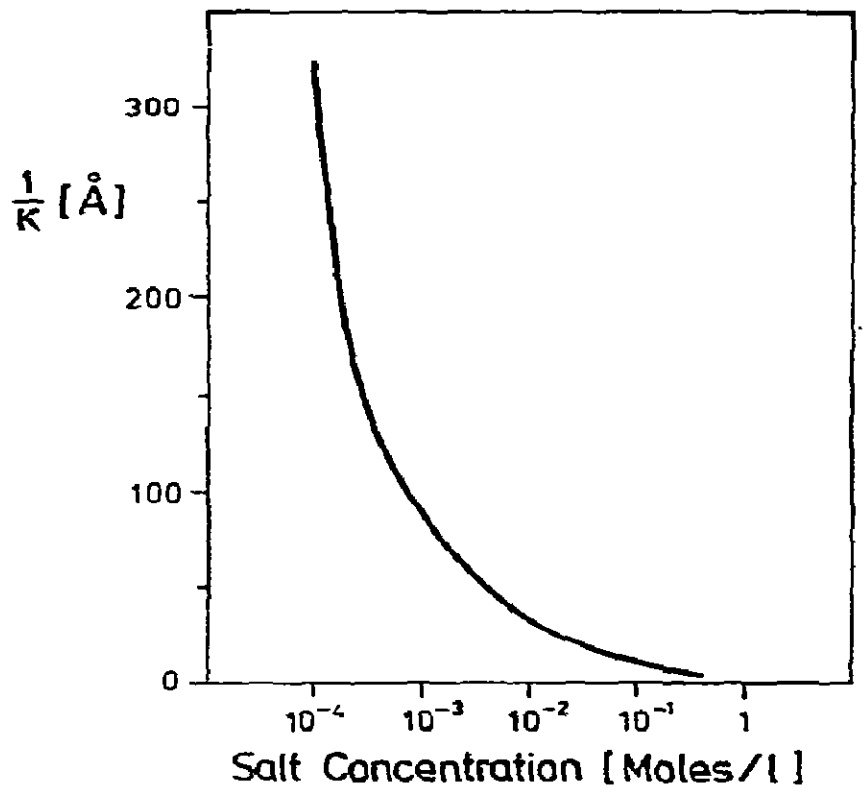

Fig. 2. Effect of salt concentration (1:1 electrolyte) on the thickness $1/\kappa$ of the diffuse layer near a charged membrane surface (cf. fig. 1). Calculated from eq. (10b) for $T = 300$ K.

Inserting $e = 4.803 \times 10^{-10}$(esu), $k = 1.38 \times 10^{-16}$ erg/degree we obtain for $\epsilon = 80$ and $T = 300$ K

$$\kappa\,[\mathrm{cm}^{-1}] = 3.241 \times 10^7\,(n_m)^{1/2} \qquad (10b)$$

with n_m now denoting the molar bulk salt concentration. $1/\kappa$ gives the distance from the membrane surface at which the electrical potential Ψ has decreased to about the 1/e fraction of its value at the surface Ψ_0. Fig. 2 shows the dependence of $1/\kappa$ on the salt concentration. At 10^{-4} M the diffuse layer has a thickness of about 300 Å; it decreases rapidly with increasing salt concentration and reaches unreasonably small values when $n_m \geqslant 0.1$ M.

To calculate ϕ we need to know how surface potential Ψ_0, surface charge density σ (charge per cm^2) and ionic strength are related. For a 1:1 electrolyte the Gouy–Chapman theory leads to the following expressions ★

$$\sigma = (\epsilon/2\pi)(kT/e)\,\kappa \sinh(e\Psi_0/2kT)\,, \qquad (11)$$

★ Here σ, e and Ψ_0 will arbitrarily be taken as positive. We are here concerned with the energy of electrostatic interaction, in which the signs of these quantities are without influence.

or

$$\Psi_0 = 2(kT/e)\sinh^{-1}(\sigma/c)\,. \tag{12}$$

c is defined as

$$c = (\epsilon/2\pi)(kT/e)\kappa\,, \tag{13a}$$

which after insertion of values for e, k and $\epsilon = 80$, $T = 300$ K becomes

$$c = 3.556 \times 10^4 (n_m)^{1/2}\,. \tag{13b}$$

For small potentials $\sinh x \propto x$ and therefore

$$\Psi_0 = (4\pi/\epsilon\kappa)\,\sigma\,. \tag{14a}$$

For high potentials $\sinh x \propto \frac{1}{2}\exp x$, and

$$\Psi_0 = 2(kT/e)\ln(2\sigma/c)\,. \tag{14b}$$

Fig. 3 shows the dependence of Ψ_0 on the salt concentration and the charge density according to eq. (12).

2.2.3. The charging process

We can now calculate the electrostatic free energy ϕ of one cm^2 of a charged surface. ϕ may be obtained as the work done in a hypothetical charging process (cf. Harned and Owen [31]) whereby one cm^2 of the surface is charged from zero to the final value following a pathway of equilibrium states:

$$\phi = \int_0^{\sigma} \Psi_0(\sigma')\,d\sigma'\,. \tag{15}$$

During this process the surface potential Ψ_0 increases according to eq. (12), and progressively more counterions accumulate in the diffuse layer while anions are pushed out into the bulk solution (cf. fig. 1). Expressing $\Psi_0(\sigma)$ according to eq. (12) we obtain from eq. (15) by integration

$$\phi = \sigma\Psi_0 - (\epsilon/\pi)(kT/e)^2\kappa\,\{\cosh(e\Psi_0/2kT) - 1\}\,. \tag{16}$$

Since Ψ_0 depends on the charge density σ and the salt concentration n_m, ϕ is also a function of σ and n_m. Furthermore, as we shall see in sections 4 and 5, a variation in n can often cause a change in σ.

It is shown in appendix A1 that ϕ represents the additional work that must be done to ionize the polar groups of lipid molecules assembled in a lipid layer compared with the ionization of isolated polar groups. Our expression for ϕ differs from the one derived by Verwey and Overbeek [21] ϕ_{VO} in the additional term $\sigma\Psi_0$, i.e. $\phi = \sigma\Psi_0 + \phi_{VO}$. The value of ϕ is always positive whereas ϕ_{VO} is always negative. The reason for this difference is discussed in appendix A1. The use of ϕ_{VO} in our case would lead to the wrong prediction that an increase in surface charge density "stabilizes" the membrane structure or should lead to an increase

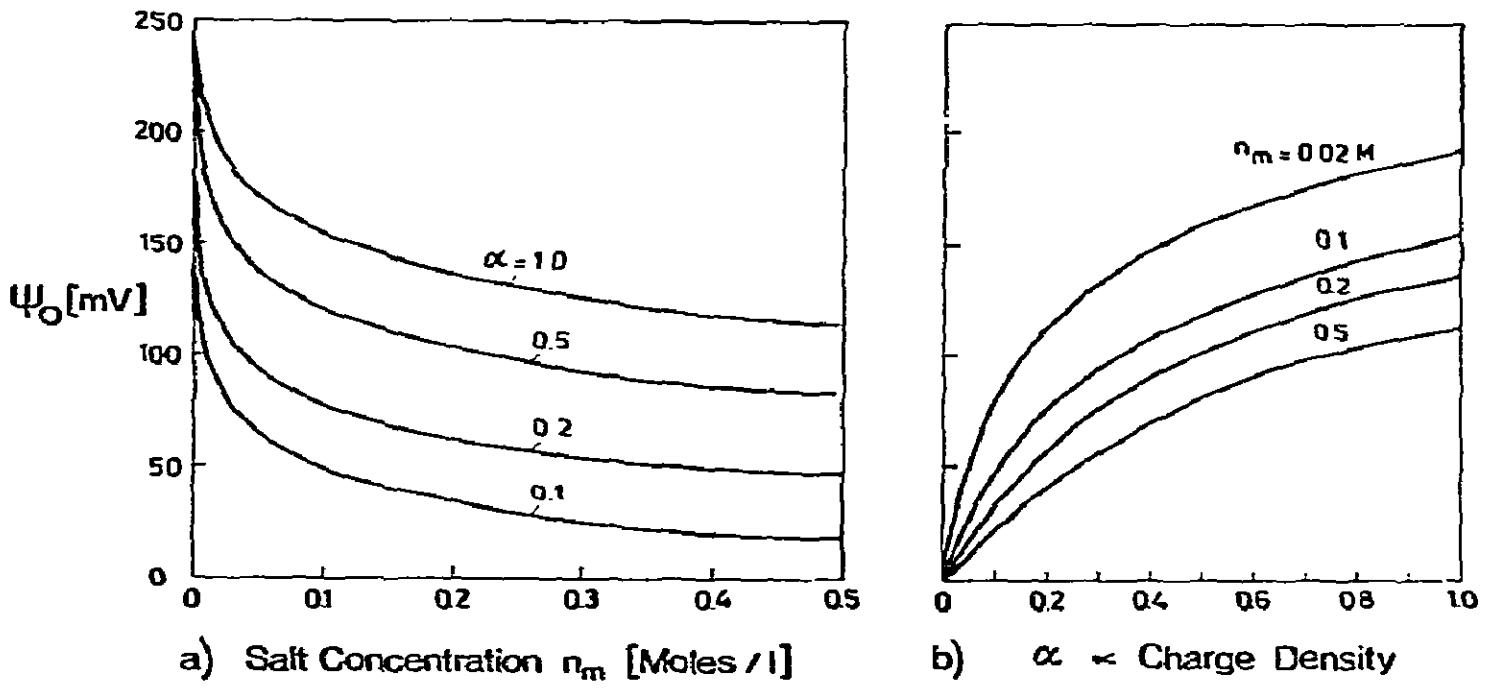

Fig. 3. Surface potential Ψ_0 at a charged lipid membrane as a function of (a) salt concentration and (b) charge density; calculated from eq. (12) for a 1:1 electrolyte at $T = 300$ K. α is the degree of dissociation of lipid molecules carrying one ionizable proton at their polar groups and occupying a molecular area of 50 A^2. $\alpha = 1$ corresponds to a charge density of one elementary charge per polar group, or 0.02 elementary charges per A^2.

of the transition temperature. This is made clear in fig. 4a.

Fig. 4b shows the variation of ϕ with the charge density for different salt concentrations. For a given value of σ, ϕ is larger at low ionic strength, where the diffuse layer is more extended (cf. fig. 2). An analogy would be a condenser of thickness $1/\kappa$ holding a constant charge: the energy stored in the condenser in-

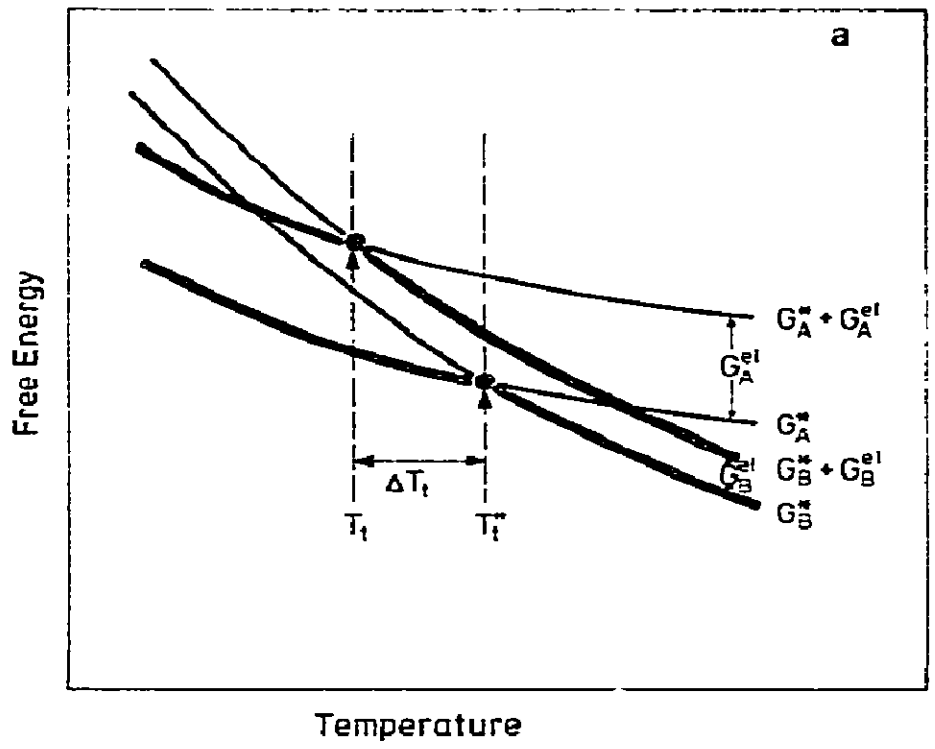

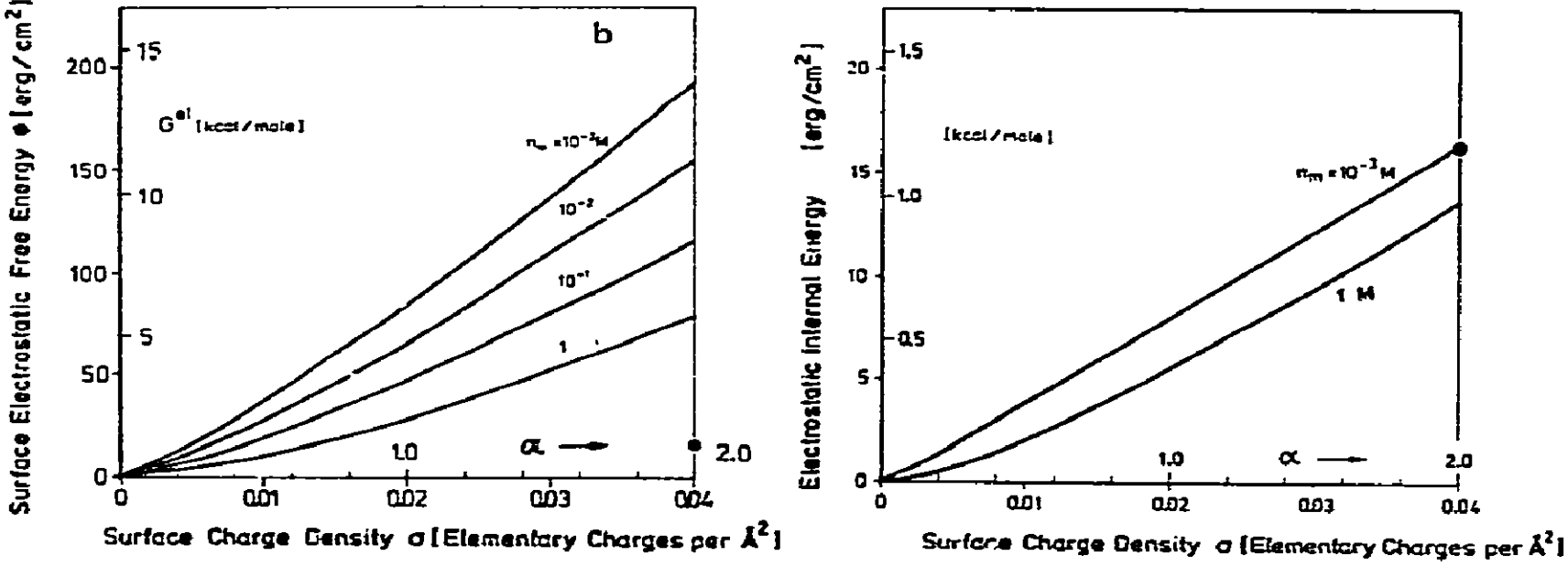

Fig. 4. (a) Temperature dependence of the free energy of ordered (A) and fluid (B) lipid membranes in the neutral and charged states. G_A^*: ordered, neutral; G_B^*: fluid, neutral; $G_A^* + G_A^{el}$: ordered, charged; $G_B^* + G_B^{el}$: fluid, charged. T_t^* and T_t are the transition temperatures of the neutral and charged forms. Below the transition the ordered phase is stabler ($G_A < G_B$), above the transition the fluid phase ($G_B < G_A$). The stabler phases are denoted by heavier curves. As is shown in the text the ordered phase has a larger electrostatic free energy ($G_A^{el} > G_B^{el}$) and therefore the charged form has a lower transition temperature (T_t). A negative sign for G^{el} would make $T_t > T_t^*$. (b) and (c) Electrostatic free energy and electrostatic internal energy as a function of the surface charge density for different salt concentrations n_m (1:1 electrolyte). *Outer axes*: the surface energy (erg/cm^2) is plotted against the charg density (elementary charges/Å^2); this plot is valid for any plane surface. *Inner axes*: valid for the case of a lipid membrane with an area per head group of 50 Å^2 and a variable degree of dissociation. Note that increasing salt concentration reduces both surface energies and that U^{el} is only about 10% of the free energy. Note the different scales of the ordinates in (b) and (c); the two dots on the right-hand ordinates mark identical energies.

creases with increasing distance between the plates. Alternatively, one may regard the membrane as a negative particle in solution which is stabilized by the preferential accumulation in its vicinity of positive ions from the neutral salt, in the manner of a Debye–Hückel electrolyte.

The curves in fig. 4b are approximately linear for a change in charge density of 20–30% which is about the change occurring at the phase transition. This justifies the use of the first-order approximation for ΔG^{el} in eq. (9).

Applying the Gibbs–Helmholtz relations to eq. (16) and assuming σ to be independent of temperature one arrives at

$$u^{el} = (\epsilon/2\pi)(kT/e)^2 \kappa \{\cosh(e\Psi_0/2kT) - 1\} \qquad (17)$$

for the surface density of the electrostatic internal energy (cf. appendix A1). $U^{el} = Lf\,u^{el}$ is the corresponding quantity per mole. As was pointed out to us by Dr. F. Jähnig of this Department (see the accompanying paper by F. Jähnig [40]) the same expression for u^{el} is obtained using the standard relationship

$$u^{el} = (\epsilon/8\pi) \int_0^\infty E^2(x)\,dx ,$$

where E is the electrical field in the diffuse layer given by $d\Psi/dx$ (cf. Overbeek [22]).

Fig. 4c shows the dependence of U^{el} on σ for $n_m = 10^{-3}$ M and 1 M. Interestingly, for given values of σ and n_m the value of U^{el} is only about 10% of that of the free energy G^{el}, indicating that the major contribution to G^{el} stems from the entropy term in $G^{el} = U^{el} - TS^{el}$.

2.2.4. *Calculation of* ΔG^{el} *and* ΔT_t

From eq. (16) we can now calculate $d\phi/df$, which is required to express G^{el} [cf. eq. (9)]. Since Ψ_0 depends on σ, eq. (16) expresses ϕ as a function of σ, which in turn depends on the packing density of the lipid molecules or on the molecular area f. Therefore

$$d\phi/df = (d\phi/d\sigma)\,d\sigma/df . \qquad (18)$$

By inspection of eq. (15) or by differentiation of eq. (16)

$$d\phi/d\sigma = \Psi_0 . \qquad (19)$$

The charge density σ can be expressed in terms of the molecular area of the lipid molecules and the charge per polar group $e\alpha$, where α denotes the degree of dissociation ($0 \leqslant \alpha \leqslant 1$), that is, the fraction of the lipids carrying a negative charge, the others being neutral, thus

$$\sigma = e\alpha/f . \qquad (20)$$

Therefore

$$d\sigma/df = -e\alpha/f^2 = -\sigma/f . \qquad (21)$$

Combining eqs. (19), (21) with eq. (18) yields

$$d\phi/df = -\Psi_0\sigma/f . \qquad (22)$$

In writing eq (18) we made use of the assumption that α is unchanged during the transition (cf. appendix A1).

Inserting the expressions for ϕ [eq. (16)] and $d\phi/df$ [eq. (22)] into eq. (9) yields

$$\Delta G^{el} = -(\epsilon/\pi)(kT/e)^2 L\,\kappa \{\cosh(e\Psi_0/2kT) - 1\}\,\Delta f , \qquad (23)$$

showing that $\Delta G^{el} = G_B^{el} - G_A^{el} < 0$, or $G_A^{el} > G_B^{el}$, i.e. the molar surface electrostatic free energy is lower in the fluid state. Since $\Delta G^{el} < 0$ and since the value of ϕ is positive we see from eq. (9) that $f\,d\phi/df$ is negative and that it is the decrease in the surface density of the electrostatic energy that gives rise to an overall decrease in the molar surface electrostatic free energy of the system at the ordered → fluid transition.

To illustrate the predictions made by eq. (23) it is useful to discuss the extreme cases of
(a) low potentials, for which $\cosh x - 1 \approx x^2/2$, and
(b) high potentials, for which $\cosh x - 1 \approx \frac{1}{2}\exp x - 1$ (cf. fig. 17). For these two cases we obtain from eq. (23):

(a) *low potentials*

$$\Delta G^{el} = -(2\pi/\epsilon)\,L(\sigma^2/\kappa)\,\Delta f , \qquad (24)$$

or

$$T_t - T_t^* = \Delta T_t = -(2\pi/e)(L/\Delta S^*)(\sigma^2/\kappa)\,\Delta f ; \qquad (25)$$

(b) *high potentials*

$$\Delta G^{el} = -2(kT/e)\,L\,\sigma\,\Delta f + (\epsilon/\pi)(kT/e)^2 L\,\kappa\,\Delta f . \qquad (26)$$

or

$$\Delta T_t = -2\frac{kT}{e}\frac{L}{\Delta S^*}\sigma\,\Delta f + \frac{\epsilon}{\pi}\left(\frac{kT}{e}\right)^2 \frac{L}{\Delta S^*}\kappa\,\Delta f . \qquad (27)$$

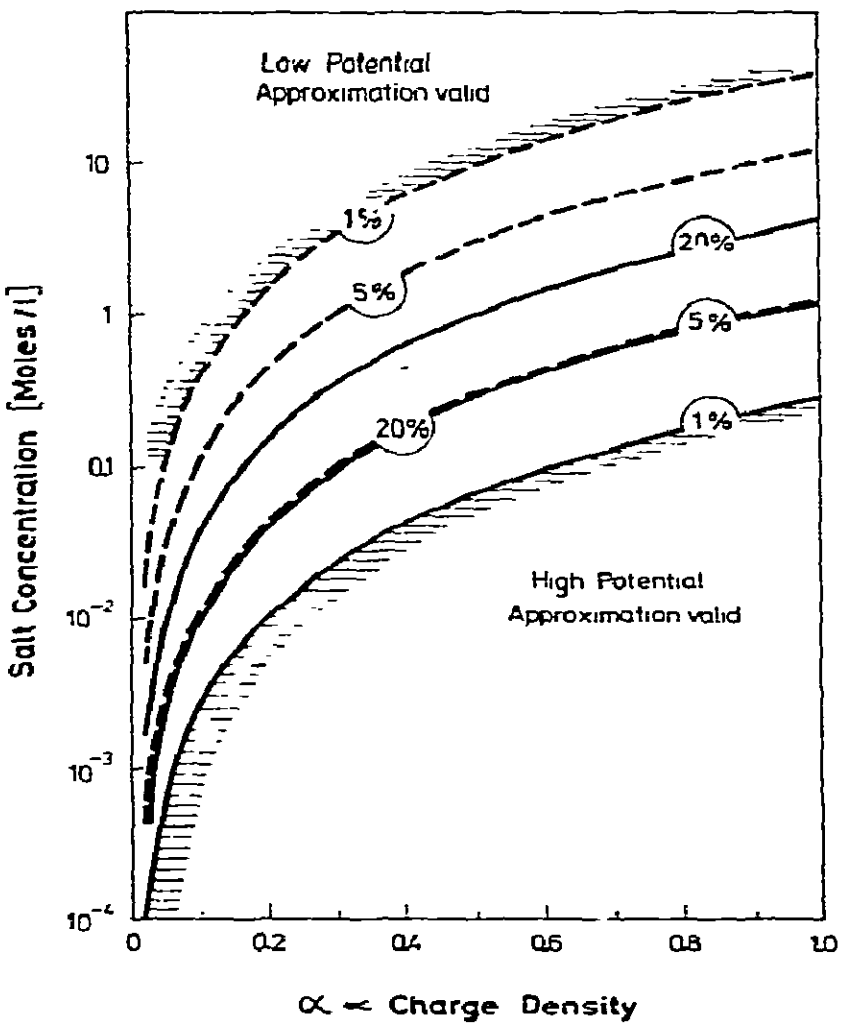

Fig. 5. Validity of low and high potential approximations for G^{el} [eqs. (24)–(27)] in terms of salt concentration and charge density (α = degree of dissociation). The curves show where the percentage error in G^{el} equals 1%, 5% and 20% when using the approximate expressions.

We recall that $\kappa \propto (n_m)^{1/2}$.

As discussed in appendix A2 these approximations can be applied only for certain ranges of the charge density σ ($= e\alpha/f$) and the salt concentration n_m. These ranges are shown in fig. 5. At the given curves the percentage error in G^{el} is 1, 5 and 20%. In our case the high-potential approximation can be used for $\alpha \gtrsim 30\%$ and $n_m \lesssim 0.5$ and therefore eq. (27) will be used extensively in the discussion of the experimental results.

The first term in this equation predicts a linear decrease in T_t with increasing charge density (in contrast, for low potentials ΔT_t is proportional to $-\sigma^2$); the second term contains the salt dependence, and predicts an increase in T_t proportional to $(n_m)^{1/2}$ (whereas for low potentials $T_t \propto -(n_m)^{-1/2}$). As will be shown there is yet another, much stronger effect of the salt concentration on T_t that operates via a change in the degree of dissociation at constant pH.

If values are inserted into eq. (27) one finds that the second term is small compared with the first one, at least for $n_m \leqslant 0.2$ M and $\alpha \geqslant 0.2$.

It is noted that the first term of eq. (27) has already been applied in a previous paper to account for results obtained on phosphatidic acid in the high-potential region (Träuble and Eibl [6]). However a rigorous derivation could not be given in that paper.

It is the purpose of the following experiments to check the predictions made by eq. (27); the strategy will be (1) to change σ at constant ionic strength, which will be done by measuring the pH-dependence of T_t, and (2) to alter the ionic strength at constant σ, which will be done at high pH where the lipids are fully ionized.

3. Materials and methods

3.1. Methylphosphatidic acid (MPA) dispersions

The experiments were performed with aqueous dispersions of dimyristoyl–MPA. This lipid has one dissociable proton per polar group with an apparent pK between 3 and 7 for salt concentrations between 0.2 and 10^{-4} M. The polar groups are negatively charged at pH $\gtrsim$ 8 and neutral at pH $\lesssim$ 2 for the salt concentrations used in our experiments.

Dispersions were prepared by shaking the weighed-out lipid with water and then incubating the mixture for at least one hour at 60°C ($T > T_t$). In addition, sonication to optical clarity for about 1 min was applied in some cases. No signs of decomposition of the lipid were observed, even after several days of incubation at neutral pH. This was confirmed by thin-layer chromatography. A gradual decomposition of MPA into the lyso-derivative and fatty acids occurs at pH values below 2 and temperatures above 50°C.

Strict precautions were taken to avoid contamination of the lipid with heavy metal ions or organic matter. Water doubly distilled from quartz was used directly from the still, and all glassware was first washed with distilled water, acetone and chloroform. Frequent checks were made to ensure that experimental results were unaffected by the addition of EDTA, showing the absence of contamination by heavy-metal ions.

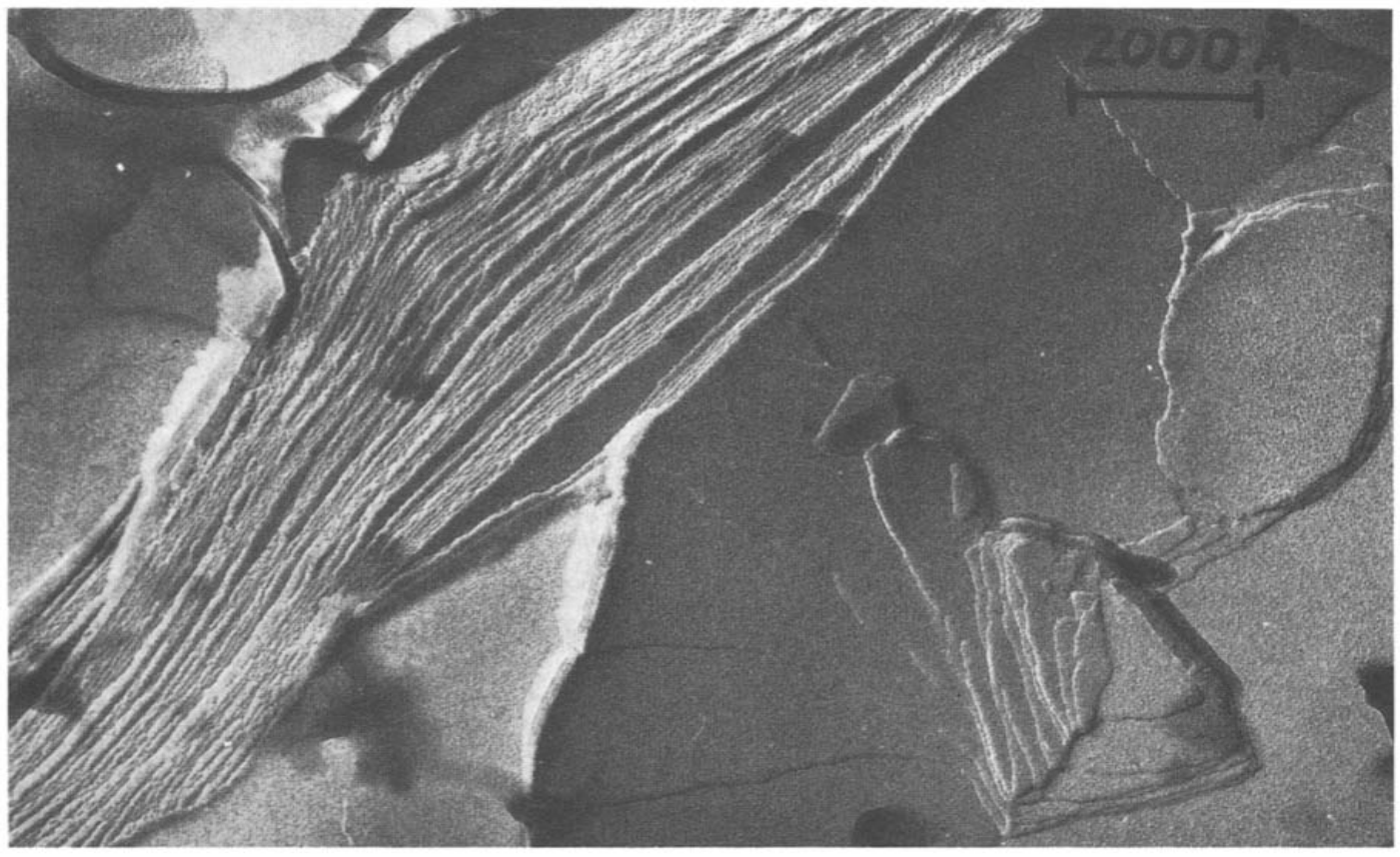

Fig. 6. Freeze fracture electron microscope picture of an MPA dispersion: Pt–Ir shadowing. MPA, 10 mg/ml not sonicated; 0.5 M NaCl; pH 8.1. Quenched from 45°C, or $T > T_t$. The upper part shows a cross-section through a stack of about 50 extended lipid lamellae; a top view of extended planar bilayers is seen in the lower part. Similar pictures are obtained when the lipid is quenched from a state $T < T_t$. This picture was kindly provided by Dipl. Phys. K. Harlos.

All salts and reagents used were of Analytical grade.

For the study of ionic interactions it is important to know what fraction of the lipid polar groups is accessible to externally added base, acid or cations. Freeze fracture experiments show that the lipid lamellae in dispersions of MPA do not form closed vesicles as in the case of lecithins but rather are organized in stacks of lamellae (cf. fig. 6), suggesting that the major part of the polar groups is accessible to externally added electrolyte. This is supported by the facts (a) that dispersions which were sonicated after the addition of electrolyte showed the same response to changes in pH and salt as dispersions without additional sonication, and (b) that binding of Ca^{2+} to salt-free dispersions of fully ionized MPA shows saturation for a lipid: Ca^{2+} ratio of 2:1 (Träuble and Eibl [7]).

3.2. Synthesis of MPA

1,2-dimyristoyl–sn-glycerol–3-phosphoric acid methyl ester, sodium salt (MPA) was synthesized by phosphorylation of 1,2-dimyristoyl–sn-glycerol (I)

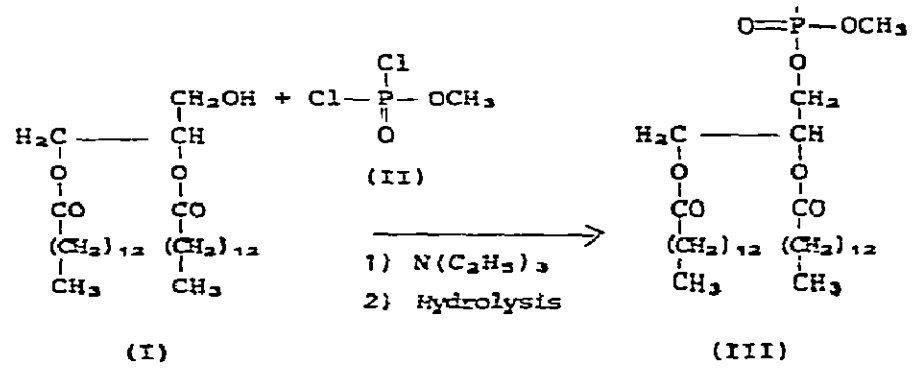

with methylphosphoric acid dichloride (II) in the presence of triethylamine (see scheme).

3.2. Methylphosphoric acid dichloride (II)

To a thoroughly stirred solution of 92 g (0.6 mole) of phosphorus oxychloride in 50 ml of tetrachloromethane in a three-necked flash equipped with a reflux condenser and a dropping funnel were added 9.6 g (0.3 mole) of methanol dissolved in 50 ml of tetrachloromethane. A continous stream of nitrogen (20 ml/

min) was directed through the reaction mixture to remove the HCl formed. After 12 hours at 25°C the solvents and the excess phosphorus oxychloride were removed by evaporation at 35°C. The residue was distilled twice and the fraction with a boiling range of 44–46°C was collected. The yield was 29 g (65%) of methylphosphoric dichloride, $CH_3-O-PO-Cl_2$, a colourless liquid.

3.2.2. MPA (III)

A solution of 14.9 g (0.1 mole) of methylphosphoric acid dichloride in 200 ml of trichloroethylene was colled in an ice bath and 15 g (0.15 mole) of triethylamine in 100 ml of trichloroethylene were added with stirring followed by the dropwise addition of 15.4 g (0.03 mole) of 1,2-dimyristoyl–sn-glycerol in 100 ml of trichloroethylene [32]. As judged by the disappearance of starting material (thin-layer chromatography) the reaction was completed after 1 hour. The solvents were removed by evaporation, the residue was dissolved in 300 ml of tetrahydrofurane and cooled with an ice bath. 200 ml of 1 N sodium acetate were added with stirring to hydrolyse the phosphochlorides. After 12 hours of hydrolysis, the pH was adjusted to 8 by the addition of 1 N NaOH. 300 ml of diisopropylether were added and mixed. After phase separation the ether phase contained the lipid and was collected. Evaporation to dryness resulted in a yellow oil, which was purified by silica gel chromatography. After evaporation of the solvents MPA was dissolved in 30 ml of chloroform and precipicated by the addition of 300 ml of acetone. The yield was 10.3 g of MPA (53%). The purity of the compound was checked by thin layer chromatography and elemental analysis (calculated for $C_{32}H_{62}NaO_8P \cdot H_2O$ (mol. wt. 646.8): C, 59.42%; H, 9.97%; P, 4.79%; found: C, 59.01%; H, 9.81%; P, 4.79%).

3.3. Phase transition measurements

The ordered ↔ fluid phase transition in dispersions of MPA was monitored using the neutral fluorescent indicator N-phenyl-naphthylamine (NPN) purchased from Eastman. The transition from the ordered to the fluid state is accompanied by a large (up to 5-fold) increase in the fluorescence intensity measured at an emission wavelength of 430 nm and an excitation wavelength of 350 nm. This increase is a result of the higher partitioning of NPN into fluid membranes, and the higher quantum yield of NPN incorporated into the membrane compared with NPN in water [33]. For an emission wavelength ⩾ 430 nm and a slit width of 0.1 mm the contribution of light scattering to the measured signal is negligibly small. Thermal transition measurements were made using an Aminco Bowman fluorimeter at heating or cooling rates of ⩽ 1°C/min. The accuracy in T_t-values is about ± 0.5°C. Typical concentrations were: lipid, 10^{-4} M; and NPN, 10^{-6} M. At these or smaller NPN/lipid ratios the indicator did not affect the lipid structure or the transition behaviour. The fluorescence properties of NPN in water are independent of pH between pH 2 and pH 9.

4. Experiments

This section presents the experimental results with a brief discussion. A quantitative comparison between theory and experiment will be performed in section 5.

4.1. pH dependence of the transition temperature

Fig. 7 shows temperature scans of the fluorescence intensity of NPN in dispersions of MPA at different pH. Apparently, in the charged state (pH ⩾ 8) the membranes have a lower transition temperature ($T_t \approx 28$°C)

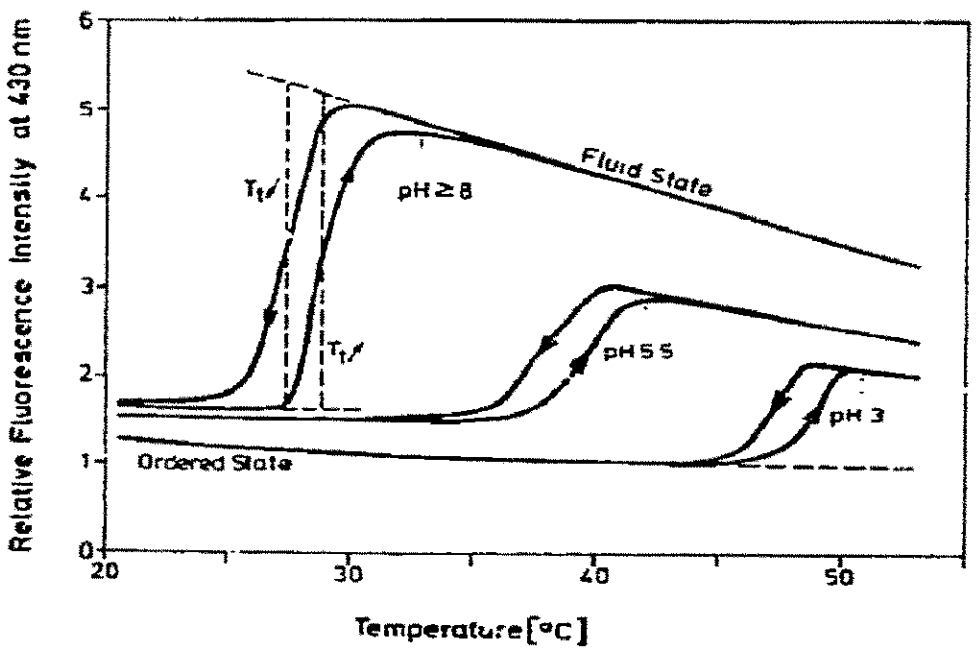

Fig. 7. Thermal transition curves for MPA at different pH values, followed by NPN fluorescence (see text). Conditions: 10^{-4} M MPA, 10^{-6} M NPN, 10^{-4} M EDTA, 5×10^{-3} M NaCl, unbuffered. The three curves were measured with the same dispersion and with identical instrument settings.

than in the neutral state ($T_t \approx 48^\circ$C at pH 3). Under the given experimental conditions the ordered → fluid transition produced a fluorescence increase by an factor of 4 at pH $\gtrsim$ 8 and by a factor of 2 at pH 3. Between 30 and 48°C the membranes are in the fluid state at pH $\geq$ 8 and in the ordered state at pH 3, and the fluorescence intensity is about four times greater in the fluid state.

Interestingly, the fluorescence intensity at pH $\geq$ 8 compared with that at pH 3 is also somewhat greater for $T < 25^\circ$C, where the membranes are always ordered and for $T > 50^\circ$C, where the membranes are always fluid. According to fig. 7 the difference is about 20% for $T < 25^\circ$C and 40% for $T > 50^\circ$C. If we attribute this difference to a closer packing of the lipid molecules in the uncharged state we must conclude that the charges cause a small expansion of the membrane even at $T < 25^\circ$C and a somewhat greater expansion at $T > 50^\circ$C.

Fig. 8 shows the effect of pH variation on the transition temperature for different salt concentrations ($0.2, 2 \times 10^{-2}, 2 \times 10^{-3}$ and 2×10^{-4} M NaCl – the latter case has an effective salt concentration of $2-3 \times 10^{-4}$ M as the 10^{-4} M counterions introduced with the lipid become important.

The values of T_t measured at increasing temperature (↑) are typically 2°C higher than the T_t-values obtained at decreasing temperature (↓); only at 2×10^{-4} M NaCl was the hysteresis greater ($\approx 5^\circ$C). In fig. 8 both values of T_t are shown for $n_m = 0.2$ M but in the other cases, to improve clarity, only T_t (↑) is given. As is seen T_t decreases with increasing pH from about 46–48°C (limiting value for low pH) to about 30°C (limiting value for high pH) within a pH range of about 2–3 units. The decrease occurs at a higher pH when the ionic strength is smaller. These curves resemble dissociation curves, and indeed, from eq. (27) it is expected that for constant ionic strength ΔT_t should be proportional to the charge density, which in turn is proportional to the degree of dissociation α.

The shift of the T_t–pH curves to higher pH values indicates an increase in the apparent pK with decreasing ionic strength. This is a general phenomenon in the dissociation of uncharged acids to yield anions, and is analogous to the effect of salts in the pH-induced helix–coil transition of poly-L-glutamic acid [1]. The qualitative explanation is that additional electrostatic work must be done in the dissociation of protons at a negatively charged surface; this work increases with decreasing ionic strength.

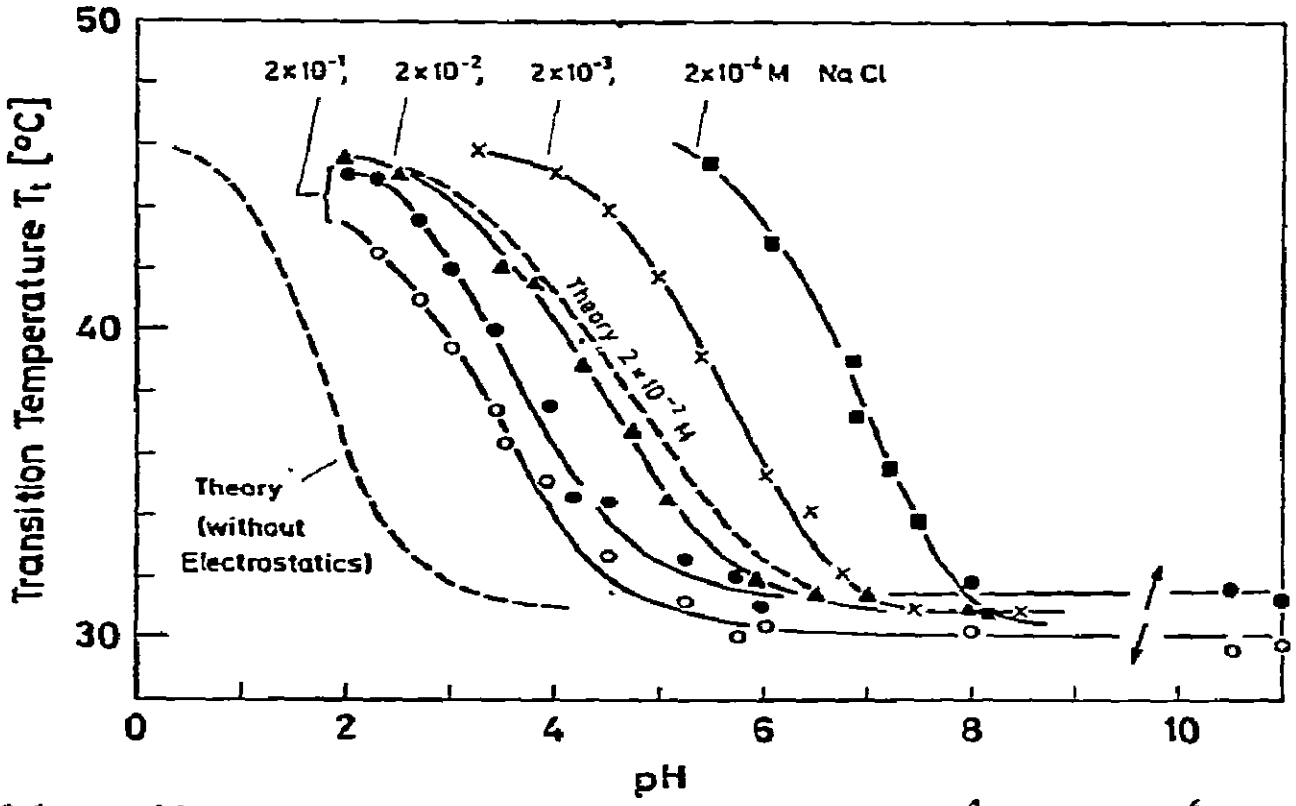

Fig. 8. Dependence of the transition temperature T_t of MPA bilayers on the pH at different salt concentrations. The T_t-values were taken from temperature scans as shown in fig. 7 measured at increasing temperature. Only for 2×10^{-1} M are shown also the values measured at decreasing temperature (↓). Conditions: 10^{-4} M MPA, 10^{-6} M NPN, unbuffered dispersions. The theoretical curve on the left was calculated without the influence of electrostatic forces on the dissociation using $pK_0 = 1.75$ (cf. section 5.1).

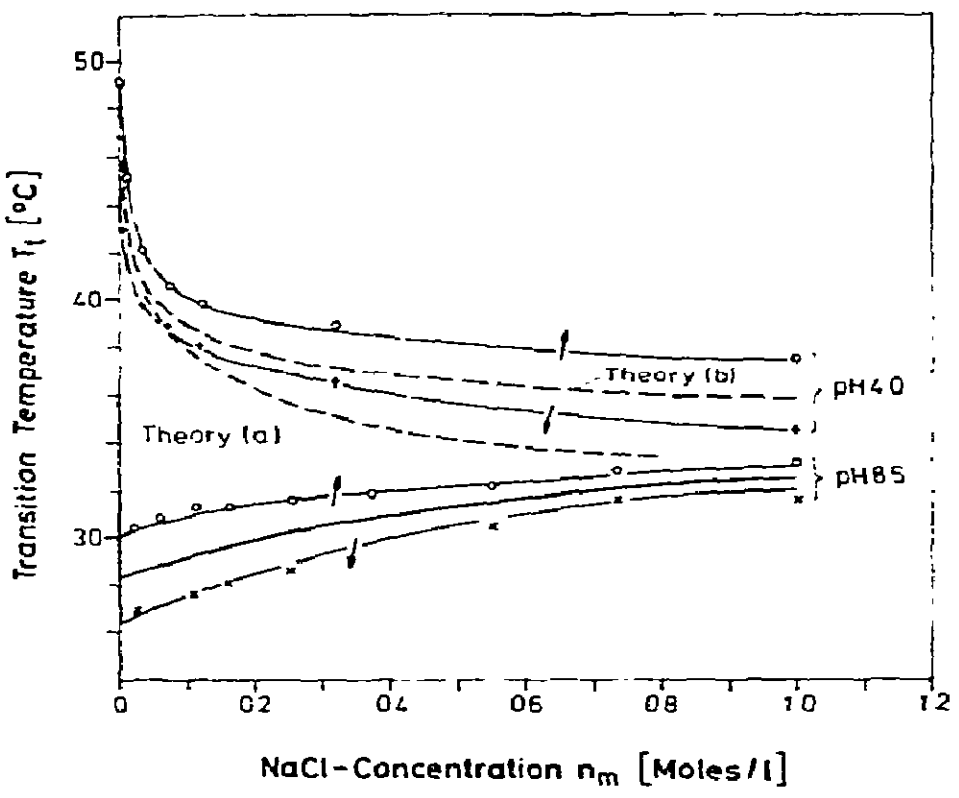

Fig. 9. Effect of NaCl on the transition temperature of MPA at low and high pH values. Symbols ↑ and ↓ denote the T_t-values measured at increasing and decreasing temperature. At pH 8.5 the lipid is always fully dissociated: addition of NaCl causes a gradual increase in T_t ("screening effect") and a decrease in hysteresis. Solid curve: mean T_t-value. At pH 4 the lipid was fully protonated at the beginning; addition of NaCl produces a rapid decrease in T_t ("enhancement of dissociation"). Conditions: 10^{-4} M MPA, 10^{-6} M NPN, 2×10^{-4} M EDTA, unbuffered. The pH was held constant throughout the experiments.

The curves in fig. 8 show that it should be possible to induce the lipid phase transition at constant temperature by a change either in pH or in salt concentration. Such transitions will be discussed in section 4.4.

4.2. Salt dependence of the transition temperature

The effect of increasing ionic strength on the transition was studied at pH 8.5, where the phosphate groups are fully dissociated (one charge per polar group) and at pH 4, where the phosphate groups are protonated at low ionic strength. As is shown in fig. 9 the addition of NaCl has quite different effects in these two cases.

At pH 8.5 the addition of salt gradually increases T_t from about 28°C to about 32°C at 1 M NaCl; at the same time the hysteresis (defined as the difference in T_t-values measured at increasing and decreasing temperature) decreases from about 4°C to 1°C.

When the values of T_t are plotted versus $(n_m)^{1/2}$ (n_m = salt concentration) one obtains a straight line with slope $\Delta T_t/\Delta(n_m)^{1/2} \approx 5\,[°C/M^{1/2}]$. The salt-induced increase in T_t shows a certain ion specificity: LiCl is more active than NaCl ($\Delta T_t/\Delta(n_m)^{1/2} = 7\,[°C/M^{1/2}]$), KCl is less active ($\Delta T_t/\Delta(n_m)^{1/2} = 3.5\,[°C/M^{1/2}]$) and CsCl has an even smaller effect.

Fig. 9 also shows that at pH 4 the addition of NaCl produces an initially sharp decrease in T_t, from about 48°C to about 40°C, which levels off at higher salt concentrations. Qualitatively, this decrease in T_t could have been predicted from fig. 8: increasing salt concentration shifted the T_t–pH curves to lower pH, so that at a given pH the transition temperature decreases with increasing ionic strength. As will be shown below, this effect results from an increase in the degree of dissociation with increasing ionic strength.

In the general case the two tendencies demonstrated by the experiments at pH 4 and pH 8.5 will be acting simultaneously, and it depends on the degree of dissociation at the beginning which of the two tendencies dominates, i.e. whether increasing salt fluidises or condenses the membrane structure.

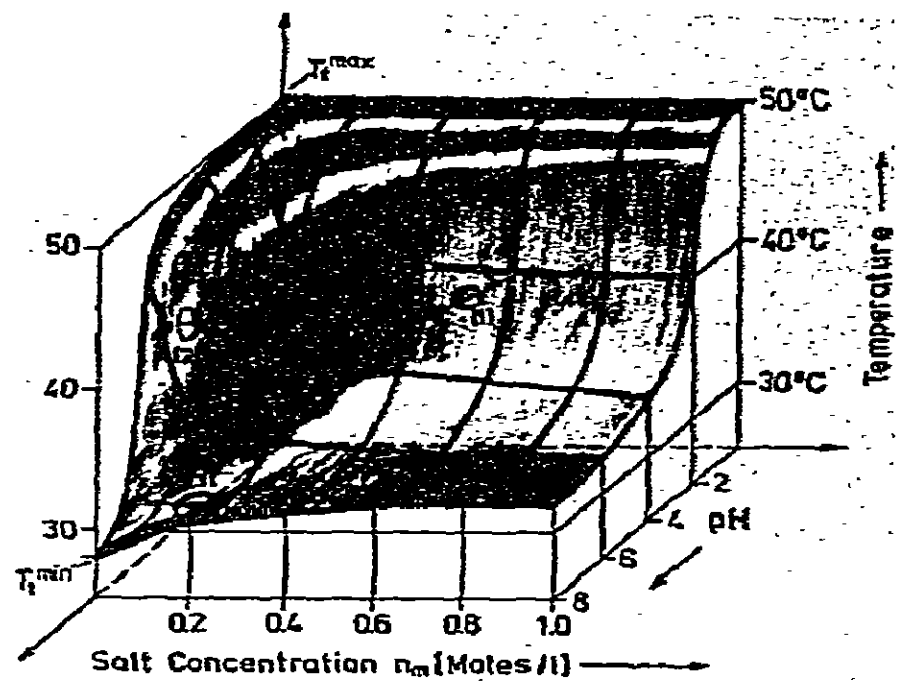

Fig. 10. Effects of pH and added salt (NaCl) on the transition temperature of MPA. The surface shows mean T_t-values and marks the boundary between the fluid state (above) and the condensed state (below) of the membrane. The arrows show various ways to induce the phase transition at constant temperature by changes in pH and salt concentration. Note: only at high pH are salt concentration and ionic strength equal.

4.3. Synopsis of pH and salt dependences

Fig. 10 shows simultaneously the effects of temperature, pH and added NaCl (n_m) on the membrane structure. This figure was constructed from the T_t–pH curves in fig. 8 and the T_t–n_m curves in fig. 9 and separates the regions of fluid and ordered membrane structure. Apparently the highest T_t-value is found at low pH without added salt (T_t^{max}), the lowest T_t-value (T_t^{min}) at high pH without added salt. These extreme values differ by about 20°C. At intermediate pH, increasing salt concentration lowers the transition temperature because of the "dissociation effect" whereas at high pH T_t increases as a result of the "screening effect". In addition from what we know already from fig. 9 this representation suggests that at low pH the salt dependence follows a sigmoid curve with a plateau at low salt concentrations. (It should be noted that only at high n_m values are salt concentration and ionic strength equal, whereas at low n_m and pH values the acid added to establish the low pH makes a significant contribution to the ionic strength.)

4.4. Induction of the transition at constant temperature

The arrows in fig. 10 indicate that in the temperature range between T_t^{min} and T_t^{max} (as defined in fig. 10) it should be possible to induce the lipid phase transition at a constant temperature, and this can be done in three different ways.

(1) For almost any salt concentration one can induce the ordered → fluid transition by an increase in pH, or the reverse transition by a decrease in pH. For example (cf. fig. 8), at 34°C and 2×10^{-2} M NaCl an increase in pH from 4 to 6 will trigger the ordered → fluid transition. Increasing salt concentration could have the following effects: (2) it should *fluidise* the membranes (ordered → fluid transition) at temperatures between $T \approx 35$°C and T_t^{max} and pH values below about pH 8; for example (cf. fig. 9) at 40°C and pH 4 the membrane is ordered for $n_m = 0.01$ M and fluid for $n_m = 0.2$ M; (3) it should *condense* the membranes (fluid → ordered transition) at temperatures between T_t^{min} and $T \approx 35$°C and pH values above pH 6 (see also fig. 9).

The following experiments illustrate these three possibilities. The transition was demonstrated, as in the case of thermally induced transitions, by measuring the change in NPN fluorescence intensity. The ordered → fluid transition is indicated by an increase, the reverse transition by a decrease in fluorescence intensity.

4.4.1. pH-induced transition

This experiment was performed at $T = 34$°C and $n_m = 2 \times 10^{-3}$ M NaCl; the initial pH was 8.0. According to fig. 8 the system is under these conditions in the fluid state, and a decrease in pH should induce the transition to the ordered state. When the pH is lowered by adding acid the fluorescence intensity decreases sharply between pH 7 and 5 and approaches a lower plateau with 20% of the initial fluorescence intensity, as one would expect from fig. 7. Fig. 11 shows the decrease in fluorescence intensity with decreasing pH, the total fluorescence change being normalized to one. The midpoint of the sigmoid transition curve is at about pH 6, in accord with the expectation from fig. 8. The transition is, of course, a consequence of charge neutralization, and the curve in fig. 11 reflects the dissociation curve. When the pH is increased again the system follows a similar curve back into the fluid state.

Similar titrations were performed at several temperatures between 20 and 60°C: for a decrease in pH from pH 8 to pH 3 the normalized fluorescence changes are similar to the curve in fig. 11. However, between 30 and 46°C the total change is about 80%, for $T > 50$°C about 40% and below 20°C only 20% or less.

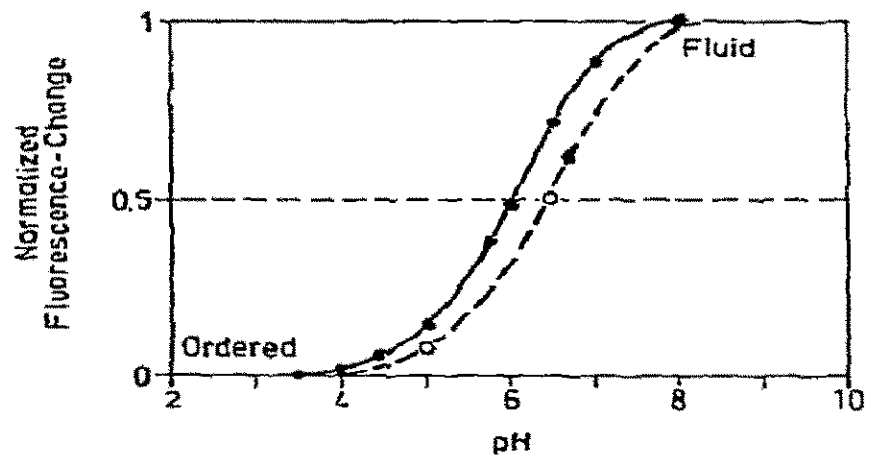

Fig. 11. pH-induced phase transition at 34°C. The fluorescence intensity of NPN at 430 nm was measured after successive additions of acid or base. The ordinate is normalized so that the difference between the fluorescence intensities at pH 8 and pH 3 equals one. The fluorescence intensity at pH 3 was about 20% of that at pH 8. Conditions: 10^{-4} M MPA, 10^{-6} M NPN, 10^{-4} M EDTA, 2×10^{-3} M NaCl.

4.4.2. Salt-induced membrane condensation

This experiment was performed at 31°C and pH 8.5 (unbuffered solution) starting with a salt-free lipid dispersion. Thus the membranes are in the fluid state at the beginning. Fig. 12 shows the change in fluorescence intensity with increasing NaCl content. After an initial plateau the fluorescence intensity shows the expected decrease at $n_m \geqslant 0.1$ M NaCl and reaches a lower plateau with about 20% of the initial intensity for $n_m \geqslant 0.8$ M NaCl. Thus the membrane condensation occurs over a broad range of the salt concentration.

4.4.3. Salt-induced membrane fluidisation

This experiment was performed at several temperatures between about 38° and 46°C with dispersions buffered at pH 4.0. Fig. 13 shows the increase in NPN fluorescence intensity which accompanied the addition of NaCl. As expected from fig. 9 more NaCl was required at lower temperatures to complete the fluidisation than at higher ones. The width of the transition for a given temperature is directly related to the steepness of the T_t–n_m curve in fig. 9 at the same temperature: the transition is the narrower, the steeper the T_t–n_m curve. A steady fluorescence reading after each NaCl addition showed that the width of the curves is not due to a kinetic effect in which equilibrium is only slowly reached.

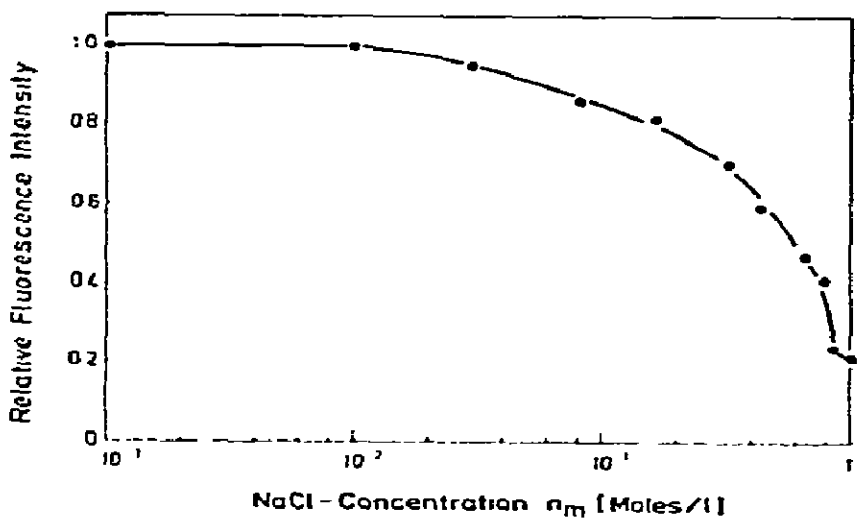

Fig. 12. Salt-induced membrane condensation (fluid → ordered transition) at 31°C and pH 8.5. The fluorescence intensity of NPN was measured at 430 nm after successive additions of NaCl. All values are corrected for dilution. This experiment represents a horizontal (= isothermal) line on fig. 9, intersecting the curve for pH 8.5. Conditions: 10^{-4} M MPA, 10^{-6} M NPN, unbuffered dispersion.

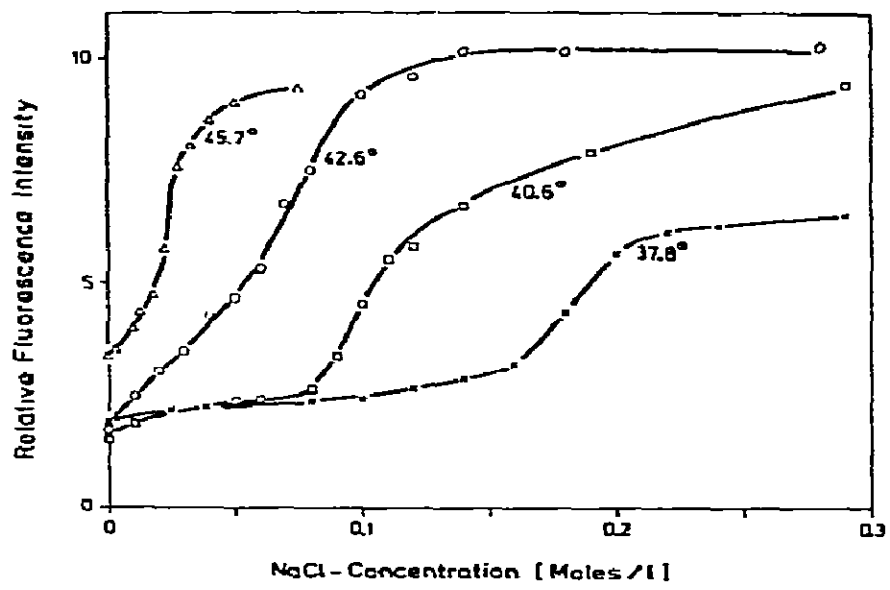

Fig. 13. Salt-induced fluidisation of MPA bilayers at pH 4 and various temperatures. Conditions: 10^{-4} M MPA, 2×10^{-6} M NPN; the pH was kept at 3.9 ± 0.1 using acetate buffer (10^{-2} M). The fluorescence intensity of NPN was measured at 430 nm after successive additions of NaCl (excitation wavelength, 330 nm). This experiment represents a series of isothermal lines on fig. 9, intersecting the curve for pH 4.

5. Comparison between theory and experiment

5.1. pH-dependence

According to figs. 8 and 10 an increase in pH, which causes the dissociation of the phosphate groups, reduces the transition temperature by about 17°C. Before we discuss the exact shape and location of the T_t–pH curves we check briefly whether the total decrease in T_t is in accord with the theory.

5.1.1. Total decrease in T_t: ΔT_t^{max}

To estimate the value of ΔT_t^{max} we use the high-potential expression for ΔT_t [eq. (27)] and neglect the last term in this equation, which is small, especially at low salt concentrations, and will be discussed below (see section 5.2.1). Thus for complete dissociation ($\sigma = e/f$),

$$\Delta T_t^{max} = -2kT(L/\Delta S^*)\,\Delta f/f\,. \qquad (28)$$

Inserting values for k, e and L, using $\Delta S^* = 17.5$ cal/mol deg (Blume [34]) we obtain for $T = 310$ K

$$\Delta T_t^{max} = -70.50\,\Delta f/f\,. \qquad (29)$$

To account for the experimental value $\Delta T_t^{max} = 17$°C we would have to take $\Delta f/f = 0.241$. From X-ray

[11, 13] and spin label [17] studies it is known that $f_A \approx 48$ Å^2 and $f_B \approx 60$ Å^2 for dipalmitoyllecithin. An X-ray study of MPA is in progress in this laboratory.

5.1.2. Shape and position of the T_t–pH curves

From eq. (27) we expect that the T_t–pH curves in fig. 8 should reflect directly the dissociation curve of the phosphate groups ($\Delta T_t \propto \alpha$). Comparison of the measured T_t–pH curves with the dissociation curve for free phosphate groups (calculated with pK_0=1.75) reveals the following main differences (cf. fig. 8): the T_t–pH curves are progressively shifted to higher pH values with decreasing salt concentration, and they are less steep.

We now calculate the T_t–pH curves using as parameters (1) the value of pK_0 to describe the dissociation in the absence of surface charge effects, and (2) the mean value of $\Delta f/f$ to describe the change in membrane area at the transition; $\Delta f/f$ will be taken to equal 0.241, as derived from the total decrease in T_t. We start from the high-potential expression for T_t, eq. (27), which is applicable for $\alpha \geqslant 0.2$ and $n_m \leqslant 0.5$. Thus

$$T_t = T_t^* - 2(kT/e)(L/\Delta S^*)e\alpha\, \Delta f/f\,, \tag{30}$$

in which we have neglected the last term in eq. (27), which is independent of α and is small for salt concentrations below 0.1 M.

Next we consider the influence of the surface charges upon the dissociation curve. In the presence of surface charges additional electrostatic work must be done in the dissociation against the charges already present. The dissociation process considered is

$$L \rightleftharpoons L^- + H^+\,, \tag{31}$$

where L and L^- denote the nonionized and ionized lipid molecules respectively. The degree of dissociation is defined as

$$\alpha = [L^-]/([L] + [L^-])\,, \tag{32}$$

where square brackets denote concentrations.

For isolated head groups we have

$$\Delta G^* = -RT \ln K_0\,, \tag{33}$$

where ΔG^* is the change in Gibbs free energy in the dissociation process and K_0 is the equilibrium dissociation constant. Neglecting activity coefficients we obtain from the law of mass action

$$\alpha = K_0/(K_0 + [H^+])\,. \tag{34}$$

At a negatively charged surface with surface potential Ψ_0 the dissociation of protons requires additional electrostatic work $Le\Psi_0$. Thus

$$\Delta G = \Delta G^* + Le\Psi_0$$

and

$$\Delta G = -RT \ln K\,.$$

The degree of dissociation is now given by

$$\alpha = \frac{K_0}{K_0 + [H^+] \exp(e\Psi_0/kT)} \tag{35}$$

instead of by expression (34) (compare ref. [35]). This equation is the direct equivalent of eq. (34) if the term $\exp(e\Psi_0/kT)$ is regarded as a Boltzmann factor giving the ratio of concentrations of free protons at the surface to those in the bulk.

Expressing Ψ_0 by eq. (14b), $\Psi_0 = (2kT/e)\ln(2\sigma/c)$, leads to

$$\alpha = \frac{K_0}{K_0 + [H^+]\,(2\sigma/c)^2}\,. \tag{36}$$

Replacing σ by $e\alpha/f$ [eq. (20)], we insert values to obtain

$$\alpha = \frac{K_0}{K_0 + 29.15\,[H^+]\,\alpha^2/n_m}\,, \tag{37}$$

with $f = 50$ Å^2, a mean value for states A and B. Rearranging gives

$$[H^+] = \{(1-\alpha)/\alpha^3\}\,K_0 n_m/29.15\,. \tag{38}$$

By considering now a series of α values we can calculate with this equation the corresponding values of $[H^+]$ or pH, i.e. the dissociation curve for a given salt concentration. The values of α can now be inserted into eq. (30) as a function of pH to calculate the transition temperature.

Such calculations were performed for different salt concentrations (n_m) using $pK_0 = 1.75$, $\Delta f/f = 0.241$ and $\Delta S^* = 17.5$ cal/deg moles (Blume [34]). The value of 1.75 for pK_0 was not arbitrarily assumed; it is implicit in the data. It can be directly obtained as shown in the next section.

A theoretical curve calculated for $n_m = 2 \times 10^{-2}$ M is shown in fig. 8; here 30°C was taken as the lower limiting value of T_t. This curve reproduces accurately the shape and the position of the measured curve. It deviates from the measured curve by a horizontal shift of only 0.25 pH units. The agreement is equally good for the other salt concentrations. Even for very small degrees of dissociation the theoretical curves calculated for high potentials do not deviate significantly from the experimental results.

5.1.3. Salt-induced shift of the T_t-pH curves

It is now easy to derive an explicit expression for the shift in the apparent pK with decreasing salt concentration. The apparent pK is the pH at which $\alpha = 0.5$ and is taken from the midpoint of the T_t–pH curves in fig. 8. Applying the condition $\alpha = 0.5$ to eq. (37) leads to

$$29.15\ [H^+]/4n_m = K_0 . \qquad (39)$$

Therefore ($K_0 = 10^{-pK_0}$)

$$pK - pK_0 = \log(29.15/4n_m) = 0.86 - \log n_m . \qquad (40)$$

As is shown in fig. 14, best agreement with the experimental results is obtained with a value of $pK_0 = 1.75$, which stands in good agreement with the values in the literature, giving

$$pK = 2.61 - \log n_m . \qquad (41)$$

For higher (lower) values of pK_0 the theoretical curve would be shifted vertically to higher (lower) pH values. (One might expect the apparent pK to tend to the value of pK_0 at very high salt concentration. This is not so for the theoretical curve in fig. 14, because for high salt concentrations the high-potential approximation is no longer valid.)

Fig. 14 demonstrates that for a charged membrane the apparent pK of the lipid head groups can be much higher than the pK of the head groups in free solution, especially at low ionic strength. Another way to read fig. 14 is that rather low proton concentrations in the bulk solution suffice to establish a much higher proton concentration, of $10^{-1.75}$ M in our case, at the membrane surface (cf. refs. [36,37]). The difference, ΔpK, between the theoretical curve and the horizontal line for $pK_0 = 1.75$ may be taken as the difference between bulk and surface pH.

For a biological membrane we may assume that about 20% of the lipids carry phosphate groups with dissociable protons. The lower curve in fig. 14 shows the difference between bulk and surface pH as a function of ionic strength for this case.

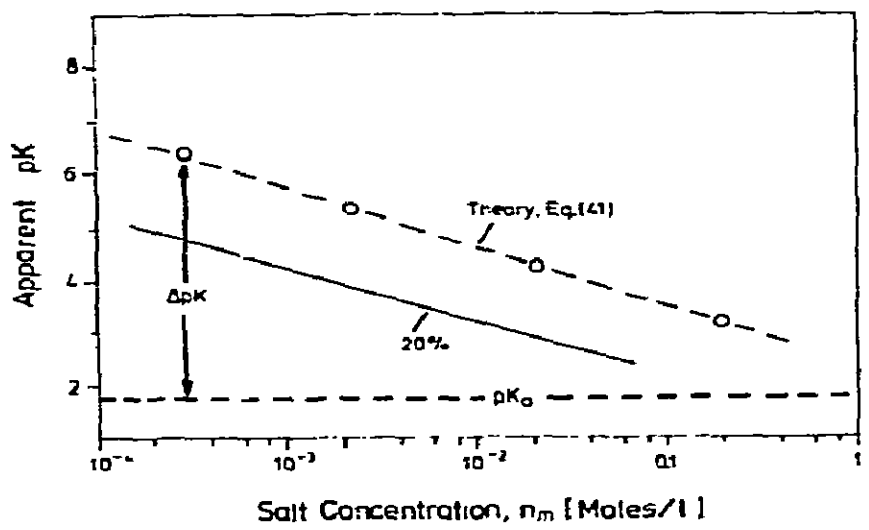

Fig. 14. Apparent pK of lipid phosphate groups at negatively charged DPPA bilayers as a function of NaCl concentration. The experimental points are taken from the T_t–pH curves in fig. 8. Theory: see section 5.1. $pK_0 = 1.75$ characterizes the dissociation in the absence of surface electrostatic effects. ΔpK equals the difference between bulk and surface pH. The curve labelled 20% shows the pK for a membrane with 20% of its lipid molecules charged.

5.2. Salt dependence

We know from fig. 9 that the addition of salt may cause either a decrease or an increase in the transition temperature, depending on the pH at which the experiment is performed. These two tendencies will now be discussed separately.

5.2.1. Increase in T_t

An increase in T_t is observed under conditions where the phosphate groups are fully dissociated so that the charge per polar group remains constant during the experiment (see fig. 9 lower curve). Under these conditions we may use the high-potential approximation for T_t eq. (27). For constant σ this equation predicts

$$T_t = T_t^{min} + (\epsilon/\pi)(kT/e)^2 (L/\Delta S^*)\, \kappa\, \Delta f , \qquad (42)$$

where T_t^{min} is defined in fig. 10.

Now

$$\kappa = 3.24 \times 10^7 (n_m)^{1/2} ,$$

i.e.

$T_t \propto (n_m)^{1/2}$.

When the measurements at pH 8.5 are plotted as T_t versus $(n_m)^{1/2}$ one obtains, in fact, a straight line with slope 5 [°C/M$^{1/2}$]. Inserting values for L, k, ϵ and e into eq. (42) and taking $\Delta S^* = 17.5$ cal/deg mole [34] we find at $T = 300$ K

$$T_t = T_t^{min} + 0.50\ \Delta f\ [Å^2]\ (n_m)^{1/2} . \qquad (43)$$

For $\Delta f = 10$ Å^2 we obtain a slope of 5 [°C/M$^{1/2}$] in satisfactory agreement with the experimental values 5 [°C/M$^{1/2}$] for NaCl and 7 [°C/M$^{1/2}$] for LiCl.

5.2.2. *Decrease in T_t*

The sharp decrease in T_t observed at pH 4 with increasing salt concentration is not explicitly contained in eq. (27). However, as may be inferred from fig. 8, this effect must be related to the salt-induced shift of the T_t–pH curves. It will be shown that the decrease in T_t can, in fact, be explained as a result of an increase in the degree of dissociation (or charge density) with increasing ionic strength. In the experiment performed at pH 4 we may presume that the phosphate groups were fully protonated at the beginning (low salt concentration), i.e. the membranes were uncharged. In the previous section we have already derived a formula that expresses the effect of increasing salt concentration on the degree of dissociation [eq. (37)]. Rearranging this we obtain

$$n_m = \beta\, \alpha^3/(1-\alpha)\,, \qquad (44)$$

where $\beta = 29.15\ [H^+]/K_0 = 0.164$ for pH 4 and $pK_0 = 1.75$.

This expression allows us to calculate α as a function of salt concentration at fixed pH. Fig. 15 is a graphical representation of the function $\alpha^3/(1-\alpha)$ $(= n_m/0.164)$. We read from this curve for a series of n_m-values the corresponding values of α. Taking $\Delta T_t^{max} = -17$°C (which coreesponds to $\Delta f/f = 0.241$ and $T_t^{max} = 48$°C we may now construct a theoretical curve for the decrease in T_t with increasing salt concentration. The curve obtained [(a) in fig. 9] predicts a somewhat larger decrease in T_t than actually observed – although it reproduces well the typical shape of the experimental salt-dependence.

However, our analysis is still incomplete, because superimposed on the dissociation-induced decrease in T_t is the salt-induced increase in T_t, discussed in the previous section. If we add to curve (a) the rising term $0.50\ \Delta f (n_m)^{1/2}$ [cf. eq. (43)] we obtain a very good representation of the experimental dependence as shown by curve (b). The shape of the theoretical curve, especially in the low-salt region, is quite sensitive to the choice of pK_0. It is therefore satisfying that the value of pK_0 found in the previous section allows us to reproduce these other experimental findings.

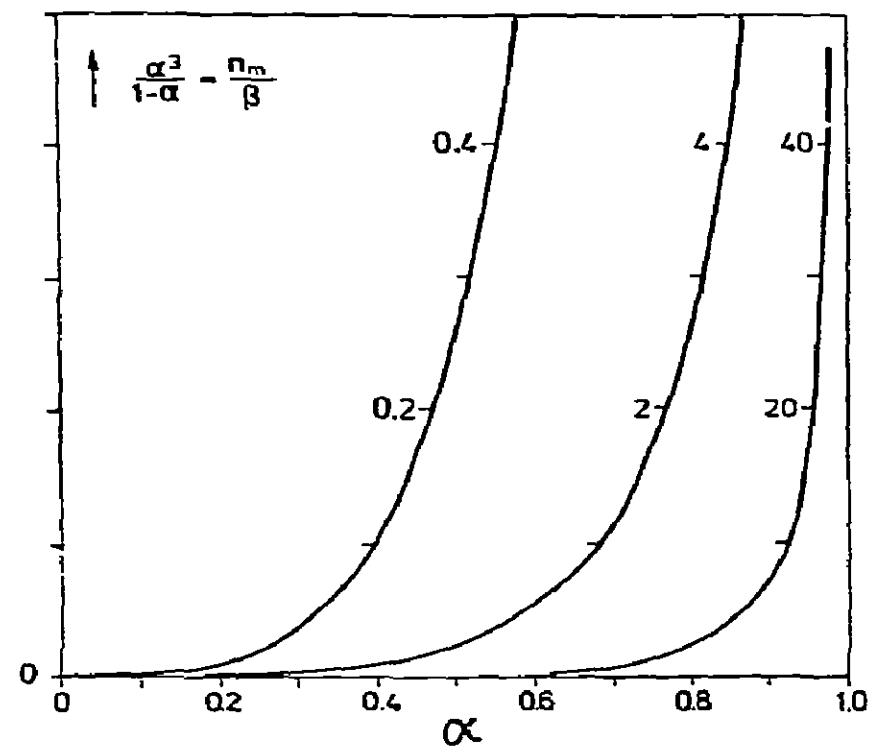

Fig. 15. Graphical solution of eq. (44). The function $\alpha^3/(1-\alpha)$ is shown on three different scales as indicated.

6. Discussion

6.1. *General conclusions*

The electrostatic free energy G^{el} associated with surface charges makes a significant contribution to the total free energy of lipid bilayers. The value of G^{el} calculated from the charging process [eq. (15)] in conjunction with the Gouy–Chapman theory is always positive; it increases with increasing charge density and with decreasing salt concentration. Thus G^{el} depends on two parameters which are important in biological systems. For a lipid membrane with a molecular area of 50 Å^2 and one charge per molecule the calculated value of G^{el} amounts to about 7 kcal/mole (or 98 erg/cm^2) at 10^{-3} M salt and 3 kcal/mole (or 42 erg/cm^2) at 0.1 M

salt. For comparison, the average energy of kinetic motion at 25°C is 0.6 kcal/mole and the energy of the hydrogen bond ranges between 3 and 7 kcal/mole; the surface energy of the air–water interface is about 70 erg/cm^2.

Interestingly, the major contribution to the value of G^{el} ($= U^{el} - TS^{el}$) stems from the entropy term; the internal energy U^{el} given by eq. (17) amounts to only 10% of the free energy. Similarly any change in G^{el}, induced for example by a change in salt concentration or the degree of dissociation, is to 90% the result of a change in the entropy term $-TS^{el}$. Therefore, although of purely electrostatic origin, the free energy G^{el} of the double layer arises mainly from the additional order established within the diffuse layer. At low salt concentration the diffuse layer extends far into the solution and G^{el} is large; at high salt concentration the diffuse layer is thinner and G^{el} is small. The usual description of the effect of added salt as a "screening effect" does not adequately express the fact that the essential physical process accompanying the addition of salt is a reduction of order within the diffuse layer near the surface. As mentioned already G^{el} decreases with decreasing charge density; therefore the electrostatic interactions tend to expand the membrane or to "fluidise" the membrane structure compared with the state for $G^{el} = 0$. Qualitatively, this tendency was demonstrated by the increase of NPN fluorescence intensity that accompanied the charging-up of the lipid membranes when the pH was increased from 3 to 9 (cf. fig. 7). Quantitatively, the effect of G^{el} on the membrane structure was studied by considering its influence on the ordered ↔ fluid phase transition of lipid membranes. The theory shows that the fluid, or expanded membrane has a lower electrostatic free energy than the ordered, or condensed state, so that the expected effect of G^{el} would be to lower the transition temperature of the system. Indeed, for MPA the appearance of one elementary charge per polar group causes a net decrease in T_t by about 20°C, i.e. about 7% of the T_t-value in Kelvin. This agrees with the theoretical prediction. (If we had used the negative value for G^{el} as derived by Verwey and Overbeek [21] then T_t would have increased with increasing charge density, compare fig. 4a.)

Because of the dependence of G^{el} on pH and ionic strength it is possible within a certain temperature range to trigger the ordered ↔ fluid phase transition at constant temperature. The arrows in fig. 10 show the different ways of doing this in the case of MPA by changes in the pH or in the salt concentration.

Practically all our experimental results can be explained by considering the work done in bringing an element of charge up to the membrane surface potential Ψ_0. To obtain the electrostatic free energy of a charged surface this work was integrated over the entire charge range. The same concept was used in section 5.1 to account for the effect of surface potential Ψ_0 on the ionization at a charged surface. Expression (12) for Ψ_0 is the only result of the Gouy–Chapman theory that enters explicitly into our calculations. In addition a simple model for the change in membrane structure at the transition was used. These two premisses will now be discussed.

6.2. *Applicability of the Gouy–Chapman theory*

Use of expression (12) for Ψ_0 has enabled us to explain the observed shift of the apparent pK with ionic strength, or the difference between bulk and surface pH (section 5.1). Expression (23) for ΔG^{el} sufficed to explain the observed pH- and salt-dependence of the transition temperature. The surface in fig. 10 which summarizes the experimental results is thus correctly described by our theoretical model.

We have to conclude that for our system the Gouy–Chapman theory – despite all its simplifications (cf. Haydon [24]) – gives a reliable value for the surface potential Ψ_0. The same conclusion was drawn by McLaughlin et al. [35] from conductance measurements on negatively charged black films. Secondly, the discrete nature of the surface charges can be neglected even when only about 10% of the lipid molecules are charged. Thirdly, our expression for G^{el} [eq. (16)] derived from the charging process [eq. (15)] has the correct positive sign and predicts correctly the observed dependence of T_t on the pH and the ionic strength. Of course, the Gouy–Chapman theory, which treats the ions as point charges, cannot account for the observed specificity of the alkali ions ($Li^+ > Na^+ \gg K^+$, Rb^+, Cs^+) in the salt-induced increase of T_t at high pH. The compensating approximations in the theory thus appear to break down when a certain size of cation is exceeded.

The conclusions drawn so far are valid only when the charged groups are sufficiently small, as in the case

of MPA. For lecithins and cephalins with more extended polar groups the situation may be different [5,6].

6.3. Criticism of our model for membrane structure and transition

Throughout this paper the lipid bilayer was considered as a system of two independent monolayers. Electrostatic interactions across the membrane were omitted. We conclude that their effect on the transition is negligible in the case of MPA bilayers.

The lipid bilayers were considered to be large, independent, planar lamellae – a view that is supported by freeze-fracture studies on MPA dispersions. Should in general a system contain small closed vesicles the following aspects would have to be taken into account: (1) possible inaccessibility of the inside polar groups to added electrolyte, (2) interactions between the diffuse layers on the inside of the vesicles, (3) (packing) differences between inner and outer surfaces and (4) effects arising from the surface curvature.

The transition was described as a lateral expansion or contraction of the membrane. The system of the hydrocarbon chains was assumed to be unaffected by the charge on the membrane; this is implicit in the use of the values T^* and ΔS^* of the uncharged membrane. Any dependence of the molecular packing on the pH must be too small to influence appreciably the T_t–pH dependence.

Under certain conditions the transition showed hysteresis; the effect was most pronounced at low salt concentration and high charge density. This suggests that the origin of the hysteresis is electrostatic in nature.

Finally, we assumed that the degree of dissociation α remains unaltered during the transition. As will be shown in a future paper this is not strictly true. In the pH region where α varies rapidly with the pH the ordered → fluid phase transition leads to an increase in α of at most a few per cent. As shown in appendix A1 these changes have no effect on the transition temperature.

Nevertheless the changes in α at the transition are of importance because they show that in addition to the influence of ionic environment upon membrane structure there exists the possibility that changes in membrane structure may alter the ionic environment. These dependences may provide a general mechanism for the coupling between membrane processes and the cell interior.

6.4. Possible biological significance

Most biological membranes are negatively charged owing to the presence of acidic lipids such as cardiolipin, phosphatidylserine, phosphatidylglycerol, etc. Therefore the electrostatic effects summarized in section 6.1 will also be operating in these systems and will be necessary for their complete physical representation – although normally they do not lead to phase transition.

The well-known effect of divalent cations as membrane "stabilizers" [38] can at least in part be understood as a decrease in G^{el} following charge neutralization by binding of these cations to negatively charged membranes. Reduction in G^{el} by 1:1 electrolyte could also be responsible for the enhanced binding of lanthanide ions to lecithins in the presence of NaCl [39].

It may be important for many membrane processes that a large difference can exist between surface and bulk pH. For our system the surface pH was up to 4 units lower than the bulk pH – depending on the ionic strength – in accord with the theory and with the results of Fromherz and Masters [36] on mixed monolayers. Typical values in the biological cell might be: ionic strength, 0.1 M; fraction of charged lipids, 20–40%. The expected difference between surface and bulk pH (cf. fig. 14) is then about 1.5 pH units. Therefore the activity of membrane-bound enzymes may differ considerably from what one would expect from the bulk pH.

Lateral phase separation. Biological membranes usually contain more than one species of lipid molecule. These molecules can form a statistical mixture or separate phases. Surface charges may play an important rôle in the lateral organization of such systems, and this rôle is quantifiable in terms of the electrostatic free energy. Consider a lipid bilayer consisting of charged and neutral lipid molecules. Using eq. (16) we can calculate the difference in electrostatic free energy for the two cases of complete mixing and complete phase separation (cf. appendix A3). As one would expect, the electrostatic free energy is always smaller for the mixed state, and therefore the difference in electrostatic free energy between the two states (separated phases minus mixed state) represents a kind of "mixing affinity"

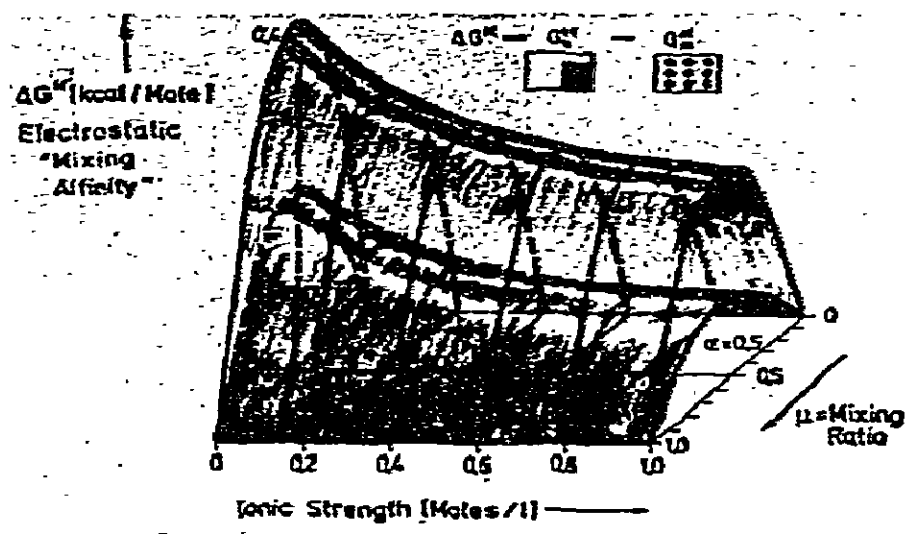

Fig. 16. Effect of the electrostatic free energy on the lateral organization of neutral and charged lipid molecules ("phase separation"). Shown is the "mixing affinity" ΔG^M as a function of the ionic strength and the fraction of charged lipids μ for different degrees of dissociation $\alpha = 0.5$ and $\alpha = 1$. The electrostatic free energy always favours the mixed state.

ΔG^M. (Again a negative sign for the electrostatic energy would predict, erroneously, that the electrostatic energy favours phase separation.) Fig. 16 shows the dependence of ΔG^M on the ionic strength and the mixing ratio μ (ratio of neutral to ionizable lipid molecules) for $\alpha = 0.5$ and $\alpha = 1$ where α equals the degree of dissociation. ΔG^M increases with decreasing ionic strength and has a maximum when ionizable and neutral lipid molecules are present in a molar ratio 1:1. For $\alpha = 1$, 0.1 M salt and a molar ratio 1:1 the electrostatic free energy of the mixed state is 0.35 kcal/mole lower than for the separated phases. For comparison, the free energy of mixing ($T\Delta S$) for an 1:1 ideal mixture ($\Delta H = 0$) is 0.416 kcal/mole.

Now let us consider the effect of the electrostatic term G^M on the lateral organization of two types of lipid molecules a and b which differ sufficiently in either chain length, degree of unsaturation or polar group structure to form separate phases in the uncharged state ($\alpha = 0$). If we now "switch on" the charges on species a, for example by an increase in pH, the resulting increased electrostatic mixing affinity ΔG^M may then suffice to produce mixing; a subsequent increase in ionic strength, which reduces ΔG^M, may cause the reverse process, leading to separate phases. Experiments with a 1:1 mixture of distearoyllecithin and MPA confirm this prediction.

To summarize: For charged membranes the electrostatic free energy tends to expand the charged surface, and thus (1) to fluidise the membrane structure, and (2) to produce lipid mixing. Therefore, by increasing (or decreasing) G^{el} of a membrane one may produce fluidisation (or condensation) of the membrane structure. For a system that is initially mixed (separated into phases) a decrease (or increase) in G^{el} can produce phase separation (or mixing).

In membranes with separated phases of neutral and charged lipid molecules large differences in surface pH will exist along the plane of the membrane; therefore enzymes incorporated into one or the other phase will operate in quite different regions of their pH-activity profile. In conjunction with the possibility of inducing phase separation by a variation in G^{el} and the preferential partitioning of enzymes into one or the other phase this opens up a multitude of possibilities for regulating the activity of membrane-bound enzymes.

Acknowledgement

We wish to thank Dr. Fritz Jähnig for valuable discussion and Dr. A. Blume of the University of Freiburg for supplying us with his unpublished calorimetric data. Many colleagues provided constructive criticism of the manuscript, particularly Dr. D. Marsh, and its preparation was greatly expedited by the cheerful efficiency of Mrs. G. Daude. This research was supported in part by the Deutsche Forschungsgemeinschaft (SFB 33). P.W. acknowledges with thanks a Research Stipend from the Alexander von Humboldt Foundation.

Appendices

A1. The electrostatic free energy

We wish here to clarify the term "electrostatic free energy" G^{el} as applied to charged membranes and to derive the change in G^{el} resulting from a change in membrane area as it occurs at the lipid phase transition.

In practice there are several ways of building up a charged surface in an aqueous solution, including: (1) compression of isolated, charged lipid molecules on a Langmuir trough to yield a highly charged surface at the lipid–water interface; (2) application of an external electrical potential difference between a mercury sur-

face and the solution; (3) chemical adsorption of ions to an (initially) uncharged surface as in the case of AgI particles, which acquire a negative charge by the adsorption of I^- ions from a HI solution; (4) stoichiometric dissociation of protons from the polar heads at a lipid bilayer surface.

In cases (1) and (2) external work must be supplied, and in case (2) this work is purely electrostatic and is given by the charging integral

$$\int_0^{\sigma} \Psi_0(\sigma')\,\mathrm{d}\sigma' . \qquad \text{(A1.1)}$$

In cases (3) and (4) the situation is more complicated because additional chemical work is involved. However, since the overall process is spontaneous the overall ΔG must be negative.

We now consider in detail the build-up of a charged lipid membrane surface by the dissociation of protons, starting from a fully protonated membrane in an unbuffered solution at pH_0. The whole process can be subdivided into a sequence of hypothetical intermediates as follows, considering one mole of lipid.

(1) Separation of the membrane into individual (protonated) lipid molecules. The work required is ΔG^s (s for separation).

(2) Dissociation of the individual molecules to a degree α; this process is characterized by a dissociation constant K_0 and is accompanied by a change in pH from pH_0 to pH_α. From standard thermodynamics one obtains for the accompanying change in free energy

$$\Delta G^{\mathrm{diss}} = RT \int_0^{\alpha} \ln\left[\frac{[H^+]}{K_0}\,\frac{\alpha'}{(1-\alpha')}\right] \mathrm{d}\alpha' .$$

(3) Hypothetical "switch-off" of the charges; the required work is ΔG^{off}.

(4) Reassembly of the molecules into a lipid membrane packed exactly as the charged membrane at the end of the whole process. The work done is ΔG^a (a for assembly).

(5) "Switch-on" of the charges (ΔG^{on}) with a concomitant build-up of the entire electrostatic interactions between the polar groups and between the charged surface and the solution. These interactions are given by the charging integral (A1.1), or by

$$\Delta G^{\mathrm{el}} = Lf \int_0^{\sigma(\alpha)} \Psi_0(\sigma')\,\mathrm{d}\sigma' ,$$

where Ψ_0 is the surface potential at any stage of the charging process and $\sigma(\alpha)$ is the final charge density corresponding to the value of α for the lipid molecules. Lf is the membrane area for one mole of lipid with a molecular area f.

Thus we obtain for the overall process

$$\Delta G = (\Delta G^s + \Delta G^a) + (\Delta G^{\mathrm{off}} + \Delta G^{\mathrm{on}}) + \Delta G^{\mathrm{diss}} + \Delta G^{\mathrm{el}} .$$

Obviously $\Delta G^{\mathrm{on}} = -\Delta G^{\mathrm{off}}$. If we further assume that the molecular packing and the local solvent structure of the charged membrane are identical to that of the protonated membrane (implying $\mathrm{d}f/\mathrm{d}\alpha = 0$) then $\Delta G^a = -\Delta G^s$ and we are left with

$$\Delta G = \Delta G^{\mathrm{diss}} + \Delta G^{\mathrm{el}} ,$$

or

$$\Delta G = RT \int_0^{\alpha} \ln\left[\frac{[H^+]}{K_0}\,\frac{\alpha'}{(1-\alpha')}\right] \mathrm{d}\alpha' + Lf \int_0^{\sigma} \Psi_0(\sigma')\,\mathrm{d}\sigma' . \qquad \text{(A1.2)}$$

At equilibrium

$$\partial \Delta G/\partial \alpha = 0 , \qquad \text{(A1.3)}$$

which yields

$$RT \ln\left[\frac{[H^+]}{K_0}\,\frac{\alpha}{(1-\alpha)}\right] + Lf\,\Psi_0(\sigma)\,\frac{\mathrm{d}\sigma}{\mathrm{d}\alpha} + \frac{\mathrm{d}f}{\mathrm{d}\alpha} \int_0^{\sigma} \Psi_0(\sigma')\,\mathrm{d}\sigma' = 0 .$$

Applying our assumption $\mathrm{d}f/\mathrm{d}\alpha = 0$, which means that the packing of the molecules is determined by the hydrocarbon chains and factors other than the charge, we obtain eq. (35) for the dissociation curve of ionizable groups at a charged surface. (The condition $\mathrm{d}f/\mathrm{d}\alpha = 0$ here applies to either state A or B of the lipid membrane, and is not in conflict with the fact that a variation in charge can trigger the phase transition at constant temperature.)

Now consider the change in ΔG that results from a change in a parameter λ (which may be the molecular area f) when α is also considered as a variable. For small variations we obtain

$$d\Delta G = \frac{\partial}{\partial\alpha}(\Delta G)\Big|_{\lambda} d\alpha + \frac{\partial}{\partial\lambda}(\Delta G)\Big|_{\alpha} d\lambda .$$

If the initial state is at equilibrium then $\partial(\Delta G)/\partial\alpha = 0$, and if we assume that K_0 is independent of λ then

$$\frac{d(\Delta G)}{d\lambda} = \frac{\partial}{\partial\lambda}(\Delta G)\Big|_{\alpha} = \frac{\partial}{\partial\lambda}\left[Lf\int_0^{\sigma}\Psi_0(\sigma')\,d\sigma'\right]_{\alpha} .$$

This shows that in the case of the lipid phase transition, where λ becomes the molecular area f, the change in ΔG is given by the change in the charging integral, as assumed in the text, and that changes in α make no contribution. The same is true for variation of any parameter in which K_0 is unaffected.

In the text we evaluated the charging integral using for Ψ_0 the Gouy–Chapman expression eq. (12). Since this expression is independent of pressure and volume, Gibbs and Helmholtz free energies are in our treatment identical. We would further mention that the final expression eq. (16) includes the repulsion between the charges on the surface. This is illustrated by regarding the charging process as formally analogous to the charging of a capacitor whose capacity is given by $d\Psi_0/d\sigma$. Here the repulsions are obviously included, and the work done in the charging process is still given by formula (15).

Let us now compare our equation (16) with the expression for the "free energy of the double layer" derived by Verwey and Overbeek [21] ϕ_{VO}. These authors considered the situation in which an initially neutral particle acquires a negative surface charge by chemical adsorption of counterions, for example AgI particles that adsorb I^- ions from an HI solution. Their expression ϕ_{VO} rests on the argument that in the final state of the adsorption process the chemical free energy difference driving the adsorption outweighs the electrical potential difference and therefore equals $-\sigma\Psi_0$ per cm^2. To this chemical term they add the purely electrical work given by the charging integral and obtain

$$\phi_{VO} = -\sigma\Psi_0 + \int_0^{\sigma}\Psi_0(\sigma')\,d\sigma' \qquad \text{per cm}^2 .$$

ϕ_{VO} is always negative and is to be understood as the total decrease in free energy during the spontaneous adsorption process. To compare this result with our expression for ΔG eq. (A1.2) we have to integrate eq. (A1.2). We do this assuming $[H^+]$ = constant, which is justified for sufficiently small concentrations of lipid. This yields

$$\Delta G^{diss} = RT\{\alpha\ln([H^+]/K_0) + \alpha\ln\alpha + (1-\alpha)\ln(1-\alpha)\}.$$

Using the equilibrium condition [eq. (A1.3)] or its explicit result [eq. (35)] we make the substitution

$$[H^+]/K_0 = \{(1-\alpha)/\alpha\exp(-e\Psi_0/kT) .$$

This yields

$$\Delta G = Lf\left[-\sigma\Psi_0 + \int_0^{\sigma}\Psi_0(\sigma)\,d\sigma\right] + RT\ln(1-\alpha) , \qquad \text{(A1.4)}$$

where we have used $\sigma = e\alpha/f$.

Written in this way it is no longer clear that for a variation in any external parameter λ the resulting change in ΔG is determined exclusively by the change in the charging integral. Formally eq. (A1.4) becomes identical with $Lf\,\phi_{VO}$ if we let $\alpha \to 0$ but keep σ fixed; this corresponds to letting $f \to 0$, i.e., to an infinite number of binding sites per cm^2. Therefore ϕ_{VO} may be taken as the decrease in free energy when a particle with an infinite number of binding sites acquires its surface charge by chemical adsorption. This approximation of the number of binding sites to infinity was implicitly made by Verwey and Overbeek [21].

We thus conclude (i) that application of this result to lipid membranes with a substantial degree of dissociation would lead to erroneous results, and (ii) that, as discussed in sections 2.2.3 and 6.1, the electrostatic free energy must be given by $Lf\phi$ [ϕ according to eq. (15)] and not by $G^{el} = Lf\phi_{VO}$.

A further limitation of the Verwey–Overbeek formula is the assumption of equilibrium with respect to the dissociation or association of charged species on the membrane surface. Our expression, in contrast, covers also cases where dissociation/association equilibrium has not yet been attained, and only breaks down where the time-scale is so small that the relaxation time of the diffuse layer becomes significant.

A2. High and low potential approximations

In section 2.2.4 we used two approximations for $\cosh x$ in eq. (23). For low potentials (case a) we approximated

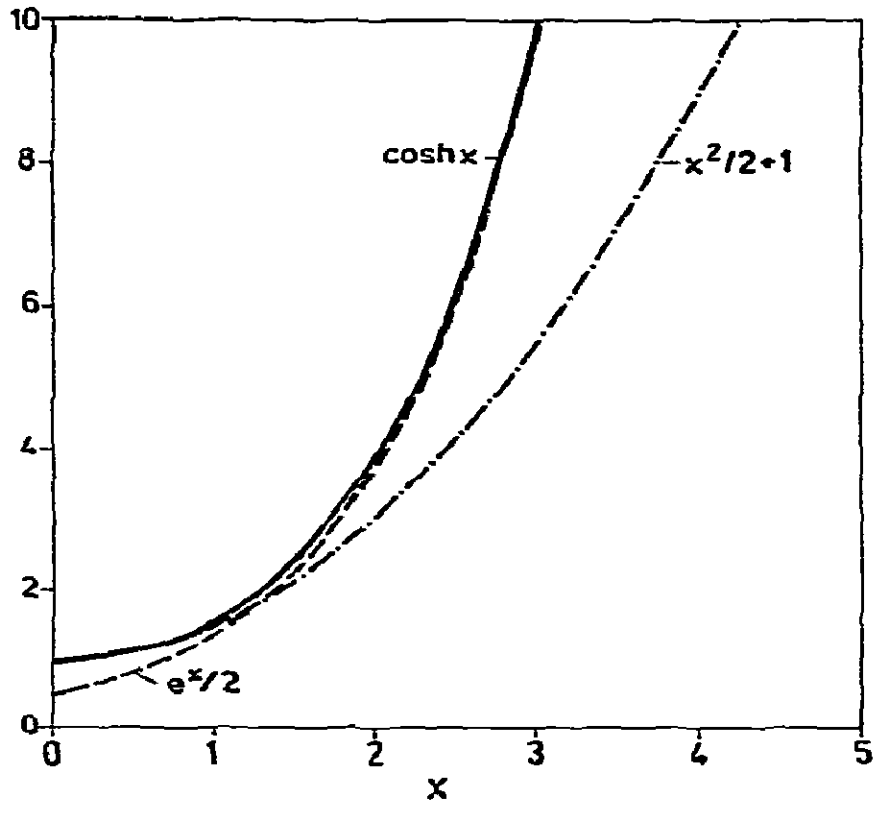

Fig. 17. Function cosh x together with approximations for low and high x-values.

$$\cosh x \approx 1 + x^2/2 \qquad \text{(A2.1)}$$

and for high potentials (case b)

$$\cosh x \approx \tfrac{1}{2} \exp x\,, \qquad \text{(A2.2)}$$

where $x = e\Psi_0/2kT$. These two approximations are compared with cosh x in fig. 17, showing that expression (A2.1) is applicable for $x \leqslant 1$ and expression (A2.2) for $x \geqslant 2$. We wish to know for which range of the charge density σ and the salt concentration n_m these approximations yield reliable values of ΔG^{el} and ΔT_t. For this purpose we calculate the contours in an n_m–α diagram at which the approximated values of ΔG^{el} deviate from the exact values by p %.

In case a these contours are determinated by the condition

$$(\cosh x - 1) - x^2/2 = p(\cosh x - 1)\,,$$

or

$$\cosh x = x^2/2(1-p) + 1\,; \qquad \text{(A2.3)}$$

and in case b

$$(\cosh x - 1) - (\tfrac{1}{2} \exp x - 1) = p\,(\cosh x - 1)\,,$$

or

$$\cosh x = (\exp x - 2)/2(1-p) + 1\,. \qquad \text{(A2.4)}$$

We now assume p = 1%, 5% and 20% and calculate the corresponding x_p-values by graphical solution of eqs. (A2.3) and (A2.4). To derive the corresponding n_m–α contours we use eq. (11) which for a given value of $x_p (= e\Psi_0/kT)$ gives a relation between σ and κ or α and n_m. The resulting curves, valid for T = 300 K and a molecular area f = 50 Å^2 of the lipid molecules, are presented in fig. 5.

A3. Rôle of G^{el} in phase separations

To quantify the effect of the electrostatic energy on the lateral organization of a mixed membrane containing neutral and charged lipids we calculate the difference in the molar electrostatic free energies for the extreme cases of (1) complete phase separation and (2) homogeneous mixing.

Let N_c = number of charged lipids, N_n = number of neutral lipids ($N_T = N_c + N_n$). We define the fraction of charged lipids as $\mu = N_c/N_T$. If the two species have equal molecular areas f, then the average areas occupied by the charged lipids in the two states are $F_s = fN_c$ in case 1 (s for separated phases), and $F_m = fN_T$ in case 2 (m for mixed). The charge densities in the two cases are $\sigma_s = e\alpha/f$ in case 1 and $\sigma_m = \mu e\alpha/f$ in case 2. Denoting with ϕ_s and ϕ_m the specific electrostatic free energies in cases 1 and 2 we can write the difference in molar electrostatic free energy between the two states as (capital M for "mixing")

$$\Delta G^M = G_s^{el} - G_m^{el}$$

$$= (L/N_T)\,(\phi_s F_s - \phi_m F_m)\,,$$

where ϕ has to be substituted according to eq. (16) and Ψ_0 is given by eq. (12). L is Avogadro's number. The calculation yields

$$\Delta G^M/L = 2kT\alpha\,\mu\{\sinh^{-1}(\sigma_s/c) - \sinh^{-1}(\sigma_m/c)\}$$

$$-(f\epsilon/\pi)(kT/e)^2\kappa\,(1-\mu)$$

$$-(f\epsilon/\pi)(kT/e)^2\kappa\,\{\mu\cosh(\sinh^{-1}\sigma_s/c)$$

$$-\cosh(\sinh^{-1}\sigma_m/c)\}\,,$$

where κ and c are given by eqs. (10b) and (13b). ΔG^M depends on the fraction μ of the charged lipids, the

salt concentration n_m and the degree of dissociation α, which was taken to be equal for states 1 and 2. As one would expect, $\Delta G^M \to 0$ for $\mu = 1$ and $\mu = 0$. ΔG^M has been evaluated numerically for $T = 300$ K, $\epsilon = 80$ and $f = 50$ Å^2. The results are presented in fig. 16, which shows ΔG^M as a function of n_m and μ for $\alpha = 0.5$ and $\alpha = 1$.

References

[1] G.D. Fasman, in: Polyamino acids, polypeptides and proteins, eds. E.R. Blout and M.A. Stahman (Univ. Wisconsin Press, Madison, 1962) p. 449.
[2] M.Th. Record Jr., Biopolymers 5 (1967) 975,993.
[3] A. Katchalsky, Polyelectrolytes, IUPAB Symposium on Maromolecules, Leyden (1970).
[4] G.S. Manning, Biopolymers 11 (1972) 937,951.
[5] H. Träuble, Biomembranes 3 (1972) 197.
[6] H. Träuble and H. Eibl, Proc. Natl. Acad. Sci. US 71 (1974) 214.
[7] H. Träuble and H. Eibl, in: Functional linkage of biomolecular systems, eds. F.O. Schmitt, D.M. Schneider and D.N. Crothers (Raven Press, New York, 1975) p. 59.
[8] K. Jacobson and D. Papahadjopoulos, Biochemistry 14 (1975) 152.
[9] A.J. Verkleij, B. de Kruyff, P.H.J.Th. Ververgaert, F.J. Tocanne and L.L.M. van Deenen, Biochim. Biophys. Acta 339 (1974) 432.
[10] D. Chapman, J. Urbina and K.M. Keough, J. Biol. Chem. 249 (1974) 2512.
[11] D. Chapman, Quart. Rev. Biophys. 8 (1975) 185.
[12] H. Träuble and D. Haynes, Chem. Phys. Lipids 7 (1971) 324.
[13] A. Tardieu, V. Luzzati and F.C. Reman, J. Mol. Biol. 75 (1973) 711.
[14] J. Seelig and W. Niederberger, Biochemistry 13 (1974) 1585.
[15] Y.K. Levine, in: Progress in biophysics and molecular biology, Vol. 24, eds. J.A.V. Butler and D. Noble (Pergamon Press, Oxford, 1972) p. 1.
[16] B.D. Ladbrooke, R.M. Williams and D. Chapman, Biochim. Biophys. Acta 150 (1968) 333.
[17] D. Marsh, Biochim. Biophys. Acta 363 (1974) 373.
[18] H.-J. Hinz and J.M. Sturtevant, J. Biol. Chem. 247 (1972) 6071.
[19] M.G. Gouy, J. Phys. 9 (1910) 457; Ann. Phys. (Paris) 7 (1917) 163.
[20] D.L. Chapman, Phil. Mag. 25 (1913) 475.
[21] E.J.W. Verwey and J.Th.G. Overbeek, Theory of the stability of lyophobic colloids (Elsevier, Amsterdam, 1948).
[22] J.Th.G. Overbeek, in: Colloid science, Vol. 1, ed. H.R. Kruyt (Elsevier, Amsterdam, 1952) p. 115.
[23] J.T. Davies and E.K. Rideal, Interfacial phenomena (Academic Press, New York, 1961).
[24] D.A. Haydon, Recent Progr. Surface Sci. 1 (1964) 94.
[25] A.W. Adamson, Physical chemistry of surfaces (Interscience, New York, 1967).
[26] A. Sanfeld, Thermodynamics of charged and polarized layers (Wiley, New York, 1968).
[27] R. Aveyard and D.A. Haydon, An introduction to the principles of surface chemistry (Cambridge Univ. Press, London, 1973).
[28] G.H. Bolt, J. Colloid Sci. 10 (1955) 206.
[29] M.J. Sparnaay, Rec. Trav. Chim. 77 (1958) 872.
[30] J.R. MacDonald and C.A. Barlow, J. Chem. Phys. 36 (1962) 3066.
[31] H.S. Harned and B.B. Owen, The physical chemistry of electrolytic solutions (Reinhold, New York, 1943).
[32] E. Baer and H.O.L. Fischer, J. Biol. Chem. 128 (1939) 475.
[33] H. Träuble and P. Overath, Biochim. Biophys. Acta 307 (1973) 491.
[34] A. Blume, Doctoral Dissertation, University of Freiburg (1976).
[35] S.G.A. McLaughlin, G. Szabo and G. Eisenmann, J. Gen. Physiol. 58 (1971) 667.
[36] P. Fromherz and B. Masters, Biochim. Biophys. Acta 356 (1974) 270.
[37] E.D. Goddard, Advan. Colloid Interface Sci. 4 (1974) 25.
[38] D.J. Triggle, in: Progress in surface and membrane science, Vol. 5, eds. J.F. Danielli, M.D. Rosenberg and D.A. Cadenhead (Academic Press, New York, 1972) p. 267.
[39] H. Hauser, M.C. Phillips, B.A. Levine and R.J.P. Williams, Europ. J. Biochem. 58 (1975) 133.
[40] F. Jähnig, Biophys. Chem. 4 (1976) 309.